Gold nanoparticles modulate the crosstalk between macrophages and periodontal ligament cells for periodontitis treatment

AUTHOR(S)

Can Ni, Jing Zhou, Na Kong, Tianying Bian, Yangheng Zhang, Xiaofeng Huang, Yin Xiao, Wenrong Yang, Fuhua Yan

PUBLICATION DATE

01-06-2019

HANDLE

10536/DRO/DU:30120770

Biomaterials 206 (2019) 115–132

Contents lists available at ScienceDirect

Biomaterials

journal homepage: www.elsevier.com/locate/biomaterials

Gold nanoparticles modulate the crosstalk between macrophages and periodontal ligament cells for periodontitis treatment

Can Ni[a,1], Jing Zhou[a,1], Na Kong[b], Tianying Bian[a], Yangheng Zhang[a], Xiaofeng Huang[a], Yin Xiao[c,**], Wenrong Yang[b,***], Fuhua Yan[a,*]

[a] Nanjing Stomatological Hospital, Medical School of Nanjing University, Nanjing, 210008, Jiangsu, People's Republic of China
[b] School of Life and Environmental Science, Centre for Chemistry and Biotechnology, Deakin University, Geelong, Victoria, 3216, Australia
[c] Institute of Health and Biomedical Innovation & the Australia-China Centre for Tissue Engineering and Regenerative Medicine, Queensland University of Technology, Brisbane, Queensland, 4059, Australia

ARTICLE INFO

Keywords:
Gold nanoparticles
Periodontitis
Macrophages
Periodontal ligament cells
Periodontal regeneration
Inflammatory microenvironment

ABSTRACT

The regeneration of lost periodontal apparatus in periodontitis treatment remains a clinical challenge due to the limited regenerative capacity of cementum, periodontal ligament and alveolar bone in periodontitis condition. For periodontal tissue regeneration, it is essential to regulate the inflammatory response and the subsequent differentiation of periodontal cells under the condition due to the infectious nature of the disease. In this study, it was noted that 45 nm gold nanoparticles (AuNPs) could exhibit significant anti-inflammatory effect and improve the periodontal inflammatory microenvironment via regulating inflammatory and regenerative cytokine production and modulating macrophage polarization, subsequently affect the differentiation of human periodontal ligament cells (hPDLCs). With the addition of direct effects of AuNPs on hPDLCs, the periodontal tissue differentiation capacity of hPDLCs in LPS-activated inflammatory macrophage-hPDLCs coculture system was significantly enhanced by the interaction between AuNPs-conditioned macrophage and AuNPs-stimulated hPDLCs. The potential therapeutic application of AuNPs in periodontal tissue regeneration and periodontitis treatment was investigated using both rat fenestration and ligature-induced periodontitis models. It was found that the treatment of 45 AuNPs showed significantly increased newly-formed periodontal attachment, bone and cementum in periodontal defect and less tissue destruction in the progression of periodontitis. This study demonstrated that 45 nm AuNPs could not only directly modulate hPDLCs, but also regulate the early inflammatory response of periodontal tissues via the regulation of macrophage phenotypes, therefore, generate a microenvironment with constraint inflammatory cytokine levels and reparative cytokines such as bone morphogenetic protein-2 (BMP-2), leading to PDLC differentiation, periodontal tissue regeneration and the prevention of periodontitis progression.

1. Introduction

Periodontitis, a bacterially induced chronic inflammatory disease, usually progressively destroys the supporting structures of teeth, including the alveolar bone, cementum, periodontal ligament and gingiva, subsequently leading to the looseness and loss of teeth [1,2]. Periodontitis is not only considered as the main cause of tooth loss in adults, but also is reported to be interrelated with systemic health by increasing the risk of many diseases such as atherosclerosis, adverse pregnancy outcomes, rheumatoid arthritis, aspiration pneumonia and cancer [1,3]. Therefore, the prevention and treatment of periodontitis are essential for general health. The therapy of periodontitis do not simply aim to control the inflammation, but more importantly, to achieve the regeneration of the lost tissues [4,5]. Among them, the alveolar bone regeneration and cementum regeneration are the two vital and challenging parts [6,7]. Cementum, a unique structure in periodontal tissues, is a thin layer of mineralized tissue covering the root surface of teeth that serves as the interface for periodontal ligament anchorage to the teeth and supports the binding between teeth and bone [7,8]. The regeneration of cementum has been a gold

* Corresponding author.
** Corresponding author.
*** Corresponding author.
E-mail addresses: yin.xiao@qut.edu.au (Y. Xiao), wenrong.yang@deakin.edu.au (W. Yang), yanfh@nju.edu.cn (F. Yan).
[1] These authors contributed equally to this paper.

https://doi.org/10.1016/j.biomaterials.2019.03.039
Received 29 January 2019; Accepted 23 March 2019
Available online 25 March 2019

standard for the reconstruction of functional periodontal tissue [8]. However, the cementum only undergo quite limited remodeling throughout life, creating a serious challenge for periodontal regeneration [9]. The conventional treatments for periodontitis usually are not able to get satisfactory outcome, as these procedures seldom provide predictable and successful periodontal regeneration [10]. The development of effective methods to successfully prevent the tissue destruction and induce the bone and cementum regeneration is important in periodontitis treatment.

In the pathological process of periodontitis, it is now understood that the initial response to the infection of microbes that resides on the root surface activates innate immune system, resulting in the release of an array of cytokines and other mediators and propagation of inflammation through the periodontal tissues, subsequently driving the bone loss and connective tissue destruction in periodontitis [11,12]. These findings indicate that the modulation of immune response might be a valuable therapeutic strategy for periodontitis. In the immune system, as macrophages play an important role in innate immunity for the first line of host defense against microorganisms and are one of the major sources of these destructive cytokines, they are found to be involved in periodontal bone damage through the phenotypic switch of alternatively activated M2 to classically activated M1 [13–15]. A recent study proved that induction of M2 macrophages could prevent the bone loss in murine periodontitis models, suggesting the crucial role of macrophage polarization in the progression of periodontitis [15]. It is known that M1 and M2 macrophage subpopulations are distinguished by secreting different cytokines and play different roles in the immune system. M1 macrophages aim to defend against the invasion of pathogens by producing inflammatory factors, such as TNF-α, IL-6, and MCP-1, while M2 macrophages secrete cytokines such as IL-10 and TGF-β to exert anti-inflammatory and angiogenic effects for tissue repair and wound healing [16–19]. In addition, macrophages are able to secret BMP-2 and directly mediate the osteogenic process [20,21]. Therefore, the behavior of macrophage may affect the processes of periodontal tissue damage and regeneration.

In periodontal ligament tissue, a population of heterogeneous cells called periodontal ligament cells (PDLCs) are reported to have “stemness” [22]. PDLCs can not only differentiate into cementoblasts and osteoblasts to form cementum and bone but also exhibit fibroblastic features, thus they are thought to be the cellular basis of natural periodontal repair and regeneration [22,23].

Gold nanoparticles (AuNPs) have gained great popularity in the biomedical field and their potential in the treatment of some diseases, such as focal cerebral ischemia-reperfusion injury and cancer is reported [24,25]. AuNPs have shown regulatory effects on macrophages and osteogenesis of stem cells and osteoblasts; however, the effects differ across studies due to the application of different particle sizes, concentration, and surface modification [6,26–32]. Although those exciting progresses have been made, it is still a grand challenge to achieve the application of AuNPs in periodontology field. An earlier study by our team has found size-dependent effects of gold nanoparticles (AuNPs) on the osteogenic differentiation of human PDLCs (hPDLCs) [6], indicating a potential application of AuNPs in periodontitis treatment. However, the regulation of periodontal immune microenvironment and the subsequent effects on periodontal tissue regeneration, especially cementum in the infectious periodontal microenvironment are essential for the application of AuNPs in periodontitis treatment. Thus further study is still needed to supported the application of AuNPs in periodontitis.

In this study, we hypothesized that whether AuNPs with different diameters could improve the periodontal inflammatory microenvironment and subsequently stimulated the periodontal regeneration through regulating the crosstalk between macrophages and PDLCs, considering the modulatory potential of AuNPs in the immune response of macrophages and PDLCs differentiation. Accordingly, we firstly investigated the regulatory effects of AuNPs with different sizes on macrophages in terms of the macrophage phenotypic switch and production of inflammatory and reparative cytokines. Then effects of AuNPs on the cementogenic and osteogenic differentiation through the regulation of macrophages and hPDLCs were studied using a macrophage -hPDLCs coculture system by conditioned medium methods. Finally, the potential application of AuNPs for periodontal regeneration and periodontitis treatment was further evaluated in periodontal fenestration and ligature-induced periodontitis rat models.

2. Methods

2.1. Synthesis and characterization of AuNPs

AuNPs were synthesized with different diameters (5, 13, 45 nm) at a concentration of 0.25 mM and then the AuNPs were capped with L-cysteine as described in previous reports [6,33]. The modified AuNPs were confirmed by dynamic light scattering (DLS) and UV–visible spectrophotometry.

2.2. Cell culture

The RAW 264.7 macrophage cell line and primary hPDLCs were used. The RAW 264.7 cells were obtained from American Type Culture Collection (ATCC, Manassas, USA). hPDLCs, the primary cells isolated from human periodontal ligament tissue, were purchased from ScienCell Research Laboratories (Catalog #2630, Carlsbad, USA). These cells were both cultured in Dulbecco's modified Eagle's medium (DMEM) (Gibco, Thermo Fisher Scientific, Waltham, USA) containing 10% fetal bovine serum (FBS) (Scien NCell) and 1% penicillin/streptomycin (HyClone, Logan, USA) at 37 °C in 5% CO_2. hPDLCs between passages 2 and 6 were used for subsequent osteogenic and cementogenic differentiation studies.

2.3. Biocompatibility, cytotoxicity and cell uptake of AuNPs by macrophages

To investigate the biocompatibility, cytotoxicity and cell uptake of AuNPs by macrophages, the RAW 264.7 cells were incubated with AuNPs with three diameters (5,13,45 nm), and the RAW 264.7 cells cultured in culture medium without AuNPs were used as the control (Ctrl) group.

The cell viability of RAW 264.7 cells was studied by CCK-8 (Dojindo Molecular Technologies, Tokyo, Japan). Cells were seeded in a 96-well plate at a density of 5.0×10^3 cells/well and incubated overnight. Then, AuNPs with three diameters (5, 13 and 45 nm) were added to the culture medium at a final concentration of 10 μM. After incubation for 1, 2 and 3 days, 10 μL of CCK-8 solution was added to each well for 2 h treatment. The absorbance of 450 nm wavelength was examined by a SpectraMax M3 microplate reader (Molecular Devices, Sunnyvale, USA).

After the incubation with AuNPs for 1 day, we used the LDH Cytotoxicity Assay (Promega Corporation, Madison, USA) to determine the cell death rate upon exposure to AuNPs according to the manufacturer's instructions.

Cells were seeded in a black 96-well plate and treated with AuNPs (5, 13, 45 nm) for 24 h. Then, the intracellular reactive oxygen species (ROS) level was determined with CellROX Green Reagent (Life Technologies, Darmstadt, Germany). Briefly, the cells were washed with PBS for three times and incubated in medium containing CellROX Reagent (5 μM) for 30 min at 37 °C. Cells were then washed with phosphate buffer saline(PBS) for three times and fixed with 3.7% formaldehyde for 15 min. The fluorescence was analyzed by a fluorescence microplate reader with the excitation set at 485 nm and the emission at 520 nm (SpectraMax M3, Molecular Devices, Sunnyvale, USA).

The uptake of AuNPs with three diameters were imaged by TEM (HT7700; Hitachi Ltd., Tokyo, Japan). Cells (2.5×10^5 cells/well) were

seeded in a 6-well plate. After 1d, the AuNPs (10 μM) were added to the medium and incubated for 3 h. Then, the cells were fixed for TEM analysis.

2.4. Effects of AuNPs on macrophage polarization, inflammatory response and BMP-2 expression

To investigate the effects of AuNPs with different diameters on the inflammatory response and phenotype switch of macrophages as well as the BMP-2 expression in macrophages, we chose *E. coli* lipopolysaccharide (LPS) as the inflammation stimulus in our study. RAW 264.7 cells were pre-incubated with 10 μM AuNPs with various diameters for 6 h. Then, LPS (20 ng/mL) was or was not added to the culture medium. The RAW 264.7 cells cultured in culture medium without treatment of AuNPs or LPS were used as Ctrl group.

After 3 h of incubation with or without LPS, the total RNA was extracted using a RNAprep pure Cell/Bacteria Kit (TIANGEN, Beijing, China) and prepared for cDNA through reverse transcription using the PrimeScript RT Reagent Kit (Takara Bio, Otsu, Japan). The gene expression of factors related to the M1 phenotype (TNF-α, IL-6, iNOS) and the M2 phenotype (IL-10, Arg-1, TGF-β) and the BMP-2 expression (primers are listed in Table 1) were analyzed by real-time PCR (ABI ViiA7, Thermo Fisher Scientific, Waltham, USA). The comparative $2^{-\Delta\Delta Ct}$ method was used to quantify the relative level of different mRNA expressions. All samples were normalized to GAPDH.

Furthermore, after incubation for 18 h, the culture media of different wells was collected and centrifuged. The concentration of TNF-α (NeoBioscience, Shenzhen, China), IL-6 (eBioscience, Thermo Fisher Scientific, Waltham, USA), IL-10 (eBioscience) and BMP-2 (R&D Systems, Minneapolis, USA) in the cell supernatants were determined using an ELISA kit according to the manufacturer's instructions. Additionally, the cells treated for 18 h were collected and used for Western blotting to assess the protein expression of iNOS (M1 marker) and Arg-1 (M2 marker) or used for flow cytometry to determine the CD86 (M1 marker) expression. For Western blotting, cells were lysed by RIPA lysis buffer (Beyotime Institute of Biotechnology) to extract proteins. The proteins were separated by SDS-PAGE and then transferred onto PVDF membranes (Millipore, Bedford, MA, USA). The membranes were blocked in 5% skim milk solution dissolved in tris buffered saline (TBS) for 1 h at room temperature, followed by incubation with primary antibodies which were diluted with TBS-Tween buffer overnight at 4 °C. The primary antibody of iNOS (#13120, Rabbit mAb, dilution ratio: 1:1000) and Arg-1(#93668, Rabbit mAb, dilution ratio: 1:1000) were purchased from Cell Signaling Technology. GAPDH (Bioworld, St. Louis, USA, #AP0063, Rabbit pAb, dilution ratio: 1:10000) was used as internal control. After four-times washes, the membranes were incubated with secondary antibodies for another 1 h at room temperature. Then the target protein bands were visualized using a chemiluminescent reagent (Merck Millipore, Darmstadt, Germany) and imaging system (LAS4000M; GE Healthcare Bio-Sciences Corp., Piscataway, USA). For flow cytometry, cells were harvested and washed with PBS for three times. Then the cells were blocked with CD16/32 (Biolegend, San Diego, USA, #101302, dilution ratio: 1:50) as 4 °C for 5min and subsequently incubated with CD86 (Miltenyi Biotec, Bergisch Gladbach, Germany, #130-102-558, dilution ratio: 1:10) or the isotype control antibody Rat IgG2b (Miltenyi Biotec, #130-103-085, dilution ratio: 1:10) for 30 min at 4 °C. After that, cells were washed with PBS and then analyzed by a flow cytometer (BD FACSCalibur, BD Bioscience, New York, USA). The data were analyzed using the FlowJo v10 software.

Based on the results of the experiments above, we selected the AuNPs with the optimum diameter from the three kinds of AuNPs.

2.5. The effects of AuNPs on osteogenic and cementogenic differentiation and osteoclastogenesis-related factors expression of hPDLCs through modulating the macrophage conditioned media in the macrophage-hPDLCs coculture system

Considering the AuNPs could be removed from the culture media of macrophages by centrifugation, the macrophage-hPDLCs coculture system was established through the conditioned medium method. The media of RAW 264.7 cells which were pre-incubated with or without the AuNPs of the selected diameter for 6 h and subsequently cultured in the absence or presence of LPS for 18 h was collected as above. Then the macrophage media was centrifuged at 14000 rpm for 30 min to remove residual AuNPs, cells and insoluble substance. The culture medium (DMEM containing 10% FBS and 1% penicillin/streptomycin) was mixed with the acquired supernatant at a ratio of 3:1 to obtain the conditioned medium (CM) for further experiments. To investigate whether AuNPs could affect the differentiation of hPDLCs through modulating the macrophage-related immune microenvironment without direct application of AuNPs in PDLCs, the differentiation of hPDLCs that incubated in different macrophage CM were evaluated and hPDLCs cultured in normal culture medium was used as normal control (NC). hPDLCs were seeded in 96-well plates at a density of 5×10^3 cells/well and divided into five groups: 1) NC group, cells cultured in normal culture medium; 2) Ctrl group, cells cultured in CM of RAW 264.7 cells untreated; 3) 45 nm group, cells cultured in CM of RAW 264.7 cells that were treated with 45 nm AuNPs; 4) LPS group, cells cultured in CM of RAW 264.7 cells that were treated with LPS; 5)

Table 1
Primer sequences.

Gene	Forward Primer sequences(5′-3′)	Reverse Primer sequences(5′-3′)
TNF-α (M)	TCTTCTCATTCCTGCTTGTGG	GAGGCCATTTGGGAACTTCT
IL-6 (M)	AGTTGCCTTCTTGGGACTGA	TCCACGATTTCCCAGAGAAC
iNOS (M)	CAGCTGGGCTGTACAAACCTT	CATTGGAAGTGAAGCGTTTCG
IL-10 (M)	ACTCTTCACCTGCTCCACTG	GCTATGCTGCCTGCTCTTAC
Arg-1 (M)	CCAGATGTACCAGGATTCTC	AGCAGGTAGCTGAAGGTCTC
TGF-β (M)	CTTCAGCCTCCACAGAGAAGAACT	TGTGTCCAGGCTCCAAATATAG
BMP-2 (M)	TGAGGATTAGCAGGTCTTTGC	GCTGTTTGTGTTTGGCTTGA
RUNX-2 (H)	GGAGTGGACGAGGCAAGAGTTT	AGCTTCTGTCTGTGCCTTCTGG
ALP (H)	GACCCTTGACCCCCACAAT	GCTCGTACTGCATGTCCCCT
COL-1 (H)	AGAACAGCGTGGCCT	TCCGGTGTGACTCGT
OCN (H)	GGCAGCGAGGTAGTGAAGAG	GATGTGGTCAGCCAACTCGT
CAP (H)	CTGCGCGCTGCACATGG	GCGATGTCGTAGAAGGTGAGCC
CEMP-1 (H)	GGGCACATCAAGCACTGACAG	CCCTTAGGAAGTGGCTGTCCAG
RANKL (H)	GGCTCATGGTTAGATCTGGC	TGACCAATACTTGGTGCTTCC
OPG (H)	TCAAGCAGGAGTGCAATCG	AGAATGCCTCCTCACACAGG
GAPDH (M)	ATCACTGCCACCCAGAAG	TCCACGACGGACACATTG
GAPDH (H)	CGCTCTCTGCTCCTCCTGTT	CCATGGTGTCTGAGCGATGT

M = murine, H = human.

LPS + 45 nm group, cells cultured in CM of RAW 264.7 cells that were treated with 45 nm AuNPs and LPS. After cultured overnight, the culture medium was replaced with different CM according to the grouping situation. On days 1, 3, 5 and 7, the CCK-8 assay was used to determine the cell proliferation and viability.

To evaluate the osteogenic and cementogenic differentiation of hPDLCs, cells seeded in 6-well plates (2.5×10^5 cells/well). Then the cells were incubated with corresponding CM supplemented with the ingredients of the osteogenic differentiation medium; these ingredients included dexamethasone (0.1 μM), ascorbic acid (50 μg/mL) and β-glycerophosphate (10 mM). After 5 days, the mRNA expression of the osteogenic factors ALP, Runx-2, COL-1, and OCN and the cementogenesis-specific markers CAP and CEMP-1, as well as the osteoclastogenesis-related factors nuclear factor-kappa B ligand (RANKL) and OPG was measured by real-time PCR (primers are listed in Table 1).

On day 7, the Western blotting, ALP activity and ALP staining assays were performed. The protein levels of ALP (Santa Cruz Biotechnology, Santa Cruz, USA, #sc-365765, Mouse mAb, dilution ratio: 1:200), Runx-2 (Cell Signaling Technology, #12556, Rabbit mAb, dilution ratio: 1:1000), COL-1 (Abcam, Cam bridge, UK, # ab6308, Mouse mAb, dilution ratio: 1: 800), CAP (Santa Cruz, #sc-53947, Mouse mAb, dilution ratio: 1:400), and CEMP-1 (Abcam, #ab134231, Rabbit pAb, dilution ratio: 1:500) were evaluated by Western blotting. The Alkaline Phosphatase Assay Kit (Beyotime Institute of Biotechnology) and BCIP/NBT Alkaline Phosphatase Staining Kit (Beyotime Institute of Biotechnology) were used to determine the ALP activity and to perform ALP staining, respectively. In detail, for ALP activity, cells were lysed by 1% Triton X-100 (Sigma-Aldrich) and centrifuged to obtain the supernatant. Then the p-nitrophenol, samples and pNPP were added into a 96-well plate according to the manufacturer's instructions and incubated at 37 °C for 5–10 min, protected from light. Finally, stop solution was added and absorbance under 405 nm was read. As for ALP staining, the cells were washed with PBS and then fixed with 4% paraformaldehyde for 30 min. Then, cells were stained according to the manufacturer's instructions.

Furthermore, the alizarin red S (ARS) staining and Von Kossa staining were also used in our study to reveal the mineralization nodules of hPDLCs cultured in CM with osteogenic components for 21 days. For Alizarin Red Staining, cells were washed with PBS and fixed with 4% paraformaldehyde for 30 min. Then stained the cells with 2% alizarin red S staining solution (Sigma-Aldrich) for 5–10min. For Von Kossa staining, fixed cells were successively treated with 5% silver nitrate (Sigma-Aldrich) solution under ultraviolet light for 1 h and 10% sodium thiosulphate (Sigma-Aldrich) for 5 min.

2.6. In LPS-activated inflammatory condition, effects of AuNPs on osteogenic and cementogenic differentiation and the osteoclastogenesis-related factors expression of hPDLCs through directly modulating the hPDLCs in the macrophage-hPDLCs coculture system

To investigate the direct effects of AuNPs on hPDLCs in inflammatory microenvironment without considering the regulatory effects on macrophage CM, the CM of RAW 264.7 cultured with LPS was harvested and the CM of RAW 264.7 untreated was used as control. The hPDLCs were divided into four groups: 1) Ctrl group: cells cultured in CM of RAW 264.7 cells untreated; 2) Ctrl-AuNPs group: cells cultured with 45 nm AuNPs in CM of RAW 264.7 cells untreated; 3) LPS group: cells cultured in CM of RAW 264.7 cells that were treated with LPS; 4) LPS-AuNPs group: cells cultured with 45 nm AuNPs in CM of RAW 264.7 cells that were treated with LPS. Then the osteogenic and cementogenic function of hPDLCs were assessed as above.

2.7. In LPS-activated inflammatory condition, effects of AuNPs on osteogenic and cementogenic differentiation and osteoclastogenesis-related factors expression of hPDLCs through modulating both macrophage CM and hPDLCs in the macrophage-hPDLCs coculture system

To comprehensively estimate whether AuNPs could regulated the regenerative potential of hPDLCs on bone and cementum under inflammatory condition *in vitro*, the effects of AuNPs on macrophage CM and hPDLCs were combined. The CM of RAW 264.7 cells treated with or without AuNPs in the presence of LPS were collected and the CM of RAW 264.7 cells untreated was used as control. The hPDLCs were divided into three groups as follows: 1) Ctrl group, cells were cultured in CM of RAW 264.7 untreated; 2) LPS group, cells were cultured in CM of RAW 264.7 cells that were treated with LPS; 3) LPS + 45 nm-AuNPs group, cells were cultured with 45 nm AuNPs in CM of RAW 264.7 cells that were treated with 45 nm AuNPs and LPS. Then the cells were treated and analyzed using the methods same as above.

2.8. The in-vivo periodontal regeneration potential of the hPDLCs in AuNPs-modulated inflammatory macrophage-hPDLCs coculture system in a rat periodontal fenestration defect model

To further verify the *in-vitro* results and evaluate the *in-vivo* regenerative potential of the macrophage-hPDLCs coculture system that modulated by AuNPs in inflammatory condition, the cells were treated and used for tissue engineering in a rat periodontal fenestration defect model. The collagen membrane-hPDLCs compound was constructed as previous reported [34]. In brief, the Bio-Gide collagen membranes (Geistlich, Switzerland) were cut into 5 × 2 mm pieces and each piece was seeded with about 1×10^4 cells in a 24-well plates. After cultured in the culture medium overnight, the membrane-cell compounds were divided into 3 groups and treated as above: 1) Ctrl group, cells were cultured in CM of RAW 264.7; 2) LPS group, cells were cultured in CM of RAW 264.7 cells and treated with LPS; 3) LPS + 45 nm-AuNPs group, cells were cultured with 45 nm AuNPs in CM of RAW 264.7 cells and treated with 45 nm AuNPs and LPS. After 3 days, the compounds were collected for *in-vivo* study.

Twenty male Sprague-Dawley (SD) rats at 7weeks of age were maintained in a specific pathogen-free condition with a 12 h light/12 h dark cycle and were provided with regular sterile food and water. After fed adaptively for 1 week, the rats were anesthetized with pentobarbital sodium (Merck Millipore) via peritoneal injection. Then the rat periodontal fenestration defect was made as previous reported [7,34]. First, the right buccal skin of the rats was shaved and sterilized. Then a 2 cm-long full-thickness incision was made through the skin along the inferior border of the right mandible. The underlying masseter muscle and periosteum were dissected to expose the alveolar bone adjacent to the buccal aspect of the first and second mandibular molars. Subsequently, a periodontal fenestration defect of approximately 2 mm in width, 5 mm in length, and 1.2 mm in depth was created through grinding the alveolar bone covering on the root surfaces with round burs under saline irrigation. Residual periodontal ligament tissues and cementum on the exposed tooth root surface were removed by a sharp curette. After that, different collagen membrane-hPDLCs compounds were randomly placed into the defect of different rats with the cell side inward facing the root surface. Then a 6 mm × 3 mm collagen membrane (Sunstar, Japan) was used to cover the defect as the barrier membrane and the incision was closed by suturing. According to the group of the compounds, the rats are divided into three groups correspondingly (N = 6/group): 1) Ctrl group, compounds cultured in CM of RAW 264.7 cells untreated; 2) LPS group, compounds cultured in CM of RAW 264.7 cells treated with LPS; 3) LPS-AuNPs group, compounds cultured with 45 nm AuNPs in CM of RAW 264.7 cells treated with 45 nm AuNPs and LPS. The extra two rats without treatment were used as normal control (Normal group) for the observation of normal periodontal tissues. Three weeks after the surgery, all rats were sacrificed

by overdose with anesthetics. The right mandibles were collected for the histological examination to observe the periodontal tissue regeneration. Thin sections(4 μm) of the dental and periodontal tissues in bucco-lingual direction were harvested according to the following procedure: fixing, decalcification, dehydration, transparentizing, embedding and finally slicing. Then, the tissue sections were stained with Hematoxylin and Eosin staining (H&E) and Masson stain. The newly-formed alveolar bone, cementum and periodontal ligament were evaluated with Image Pro Plus 6.0 software. The amount of the new bone was evaluated through dividing the area of the defect by the area of new bone. The new cementum formation was determined through dividing the length of the whole denuded root surface by the length of root surface with new cementum. And the new periodontal ligament was measured through calculating the area ratio of the collagen fibers in the area of periodontal ligament.

2.9. Intervention of AuNPs on a rat ligature-induced periodontitis model

To further estimate the preventive and therapeutic effects of AuNPs on periodontitis, a rat ligature-induced periodontitis model was used. Eighteen male SD rats at 5 weeks of age were maintained. After fed adaptively for 1 week, the rats were randomly divided into three groups (N = 6/group) as follows: 1) Ctrl group, control group with no ligation; 2) Ligature (Lig) group, rats with ligature-induced periodontitis untreated; 3) Lig-AuNPs group, rats with ligature-induced periodontitis were treated with 45 nm AuNPs. In brief, the rats were anesthetized with pentobarbital sodium (Merck Millipore) via peritoneal injection. Then silk ligatures (4-0) were tied around the cervical area of the maxillary bilateral second molars to induce the periodontitis. In order to eliminate the influence of the probable tissue destruction caused by mechanical trauma, the ligatures were also placed around the teeth in control group, but they were quickly removed once they are put in place. Subsequently, the palatal gingiva of the treated molars was injected with 100 μL of 2.5 μM AuNPs (or 0.9% NaCl solution as control in Ctrl group and Lig group) at the mesial, middle and distal sites dispersedly every three days. After two weeks, all the rats were sacrificed by overdose with anesthetics. The tissues were collected for the following analyses.

To observe the changes in morphology, quantity and quality of the alveolar bone, the maxillae were scanned using Micro-CT (SkyScan 1176, Bruker micro-CT, Kontich, Belgium). Three-dimensional (3D) digitized images and sectional images in the mesio-distal and bucco-lingual direction at different sites were reconstructed and obtained (CTvox software and DataViewer software). Additionally, the bone-related parameters including bone mineral density (BMD), bone volume (BV), tissue volume (TV), and BV/TV around the molars under ligation were measured (CTAn software). The ROI of the bone-related parameters measurement was the bone area surrounding the maxillary second molars and the teeth were excluded. The bone height around the maxillary second molars were also analyzed through measuring the distances from cement-enamel junction to the alveolar bone crest at six sites around the teeth (Image-pro-plus 6.0 software), including the mesial site in buccal/palatal side (MB, MP), central site in buccal/palatal side (B, P) and distal site in buccal/palatal side (DB, DP).

Moreover, the tissue sections in the mesio-distal direction were made according to the method described above. Then the sections were stained with H&E and Masson stain, as well as the specific tartrate-resistant acid phosphatase (TRAP) stain to evaluate the histological changes and osteoclastic activity in the periodontal tissue. The number of osteoclasts per square millimeter around the alveolar bone surface was counted and analyzed on the basis of the TARP staining images. The iNOS expression (antibody obtained from Abcam, #ab15323, Rabbit pAb) in the periodontal tissues around maxillary second molars was also measured by the immunohistochemical method. Then the quantitative analysis of iNOS expression was accomplished with Image Pro Plus 6.0 software.

All the animal experiments were approved by the Animal Ethics Committee of Nanjing University and were carried out in accordance with the National Institutes of Health guide for the care and use of Laboratory animals.

2.10. Statistical analysis

All statistical computations were performed using GraphPad Prism 6.0 software, and the statistical significance was analyzed using one-way or two-way ANOVA followed by the Tukey *post hoc test*. All the data are shown as the mean ± standard deviation (SD). The level of significance was set as $P < 0.05$.

3. Results

3.1. The size-dependent effects of AuNPs on the regulation of inflammatory response and phenotype switch of macrophages

AuNPs with different diameters (5 nm, 13 nm and 45 nm) were synthesized by the chemical reduction method and then modified by L-cysteine [6,33]. The diameters of the AuNPs were confirmed by DLS measurement (Fig. S1A). According to the results, the diameters of the resulting AuNPs were 5 nm, 13 nm and 45 nm. The AuNPs were also analyzed using UV–vis absorbance spectrophotometry. The UV–vis absorption spectra showed redshifts of the maximum with increasing diameter, with the maxima shifting to 515 nm, 520 nm and 530 nm for the 5 nm, 13 nm and 45 nm nanoparticles, respectively (Fig. S1B). Three kinds of AuNPs all show great biocompatibility in RAW 264.7 macrophage cells according to the results of CCK-8 assay (Fig. S2A), LDH cytotoxicity assay (Fig. S2B) and ROS detection (Fig. S2C). The AuNPs with three diameters all could be taken in by the macrophages quickly, and the internalized AuNPs were only found inside the intercellular vesicles in the cytoplasm of macrophage cells regardless of the AuNP size (Fig. S2).

To investigate the immunoregulatory effects of AuNPs on the inflammatory response and polarization of macrophages, the *E. coli* LPS was used to simulate an inflammatory condition. The phenotype of macrophages was determined by real-time PCR, ELISA, Western blotting and flow cytometry.

In the situation without LPS stimulation, the AuNPs not only elevated the mRNA level of M1-related factors such as TNF-α, IL-6 and iNOS but also facilitated the expression of M2-related factors, including Arg-1, IL-10 and TGF-β, in macrophages (Fig. 1A). In addition, the effect was strongest for the 13 nm AuNPs, followed by the 45 nm and 5 nm AuNPs. The ELISA results for TNF-α were consistent (Fig. 1B). However, when facing the inflammation resulting from LPS, the AuNPs showed great anti-inflammatory potential. According to the real-time PCR results (Fig. 1C), the LPS stimulation could lead to extremely high expression of TNF-α, IL-6 and iNOS, and this effect could be remarkably inhibited by 13 nm and 45 nm AuNPs. Moreover, the transcription of Arg-1, IL-10 and TGF-β influenced by 13 nm and 45 nm AuNPs became more active than that in the LPS group (Fig. 1C). The role of 5 nm AuNPs was less clear and stable than other two AuNPs. ELISA results (Fig. 1D) further confirmed the effects of the 45 nm AuNPs on decreasing the concentration of the pro-inflammatory factors TNF-α and IL-6. Additionally, the IL-10 expression was enhanced by 45 nm AuNPs, but the increase was not significant (Fig. 1D). Moreover, the expression of CD86, which is a surface marker of M1-phenotype macrophage cells, was also determined by flow cytometry. The results (Fig. 1E) revealed that when LPS existed, according to the analysis results of positive rate and mean fluorescence intensity of CD86, the 45 nm AuNPs were still the only one that could depress the up-regulatory effect of LPS on CD86 expression. The expression of M2 marker CD206 was also evaluated by flow cytometry, however, the basic expression level of CD206 in RAW 264.7 cells was quite low, and the AuNP-induced changes of CD206 expression were not significant (Fig. S3). Additionally, the protein

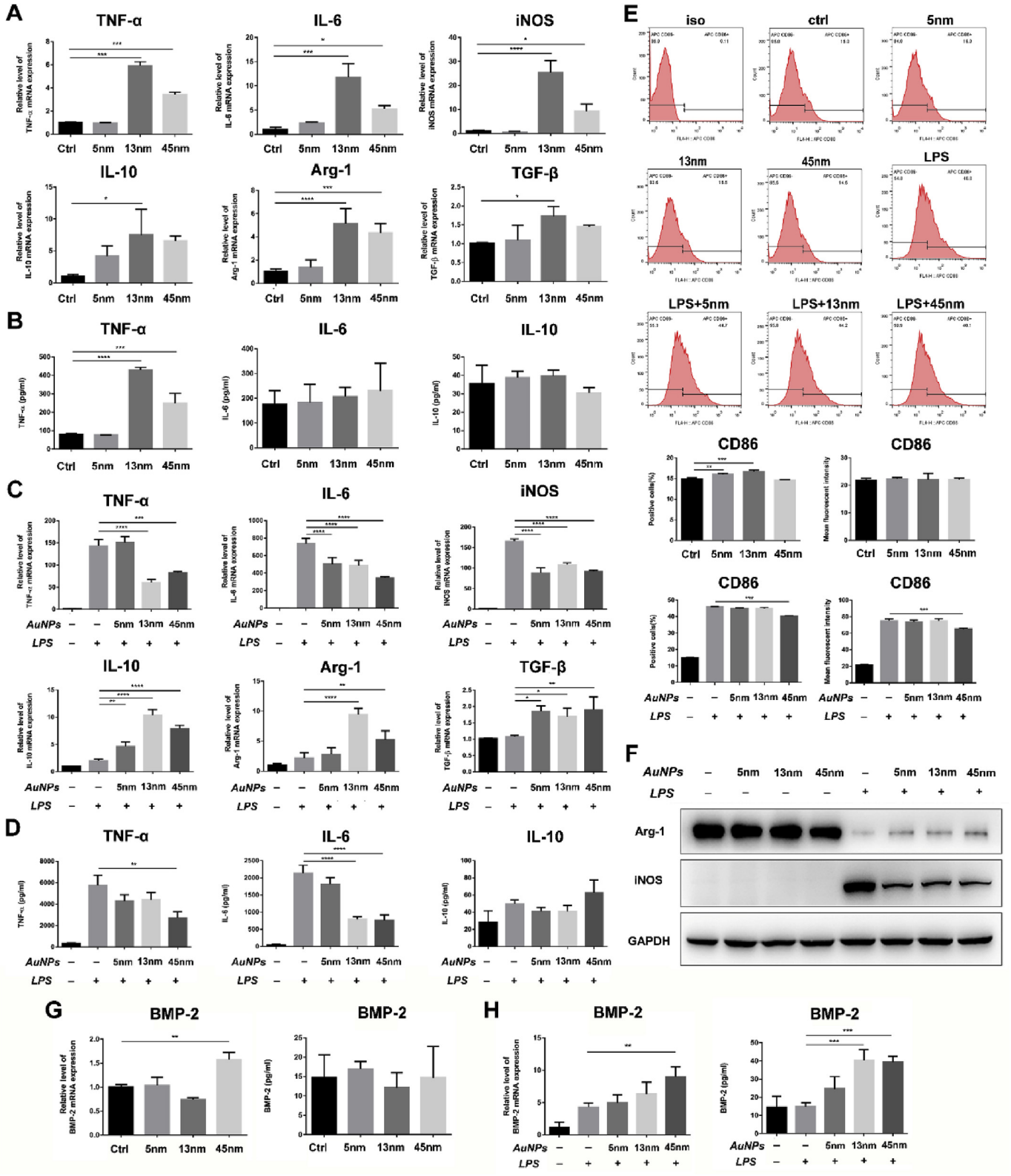

Fig. 1. AuNPs inhibited the LPS-induced inflammatory response of macrophages and promoted the macrophage phenotype switch from M1 to M2 and the expression of BMP-2. (A, C) Real-time PCR analysis of the gene expression of the M1-related TNF-α, IL-6, and iNOS and the M2-related IL-10, TGF-β, and Arg-1, (B, D) concentrations of TNF-α, IL-6 and IL-10 in the cell supernatant measured by ELISA, (E) relative protein levels of Arg-1 and iNOS determined by Western blotting, (F) flow cytometry analysis of the M1-related marker CD86 and (G, H) the BMP-2 expression measured by Real-time PCR and ELISA in RAW 264.7 cells incubated with AuNPs in the absence or presence of LPS. *P < 0.05**P < 0.01, ***P < 0.001, ****P < 0.0001.

expression of M2 marker Arg-1 and M1 marker iNOS measured by Western blotting (Fig. 1F) showed that the LPS aggravated the generation of the M1 marker iNOS and attenuated the formation of the M2 marker Arg-1, and AuNPs with the three diameters all possess the inhibitory role on the phenotypic switch in this process. Comparing with 5 nm and 13 nm AuNPs, the effects of 45 nm AuNPs still seemed to be slightly stronger (Fig. 1F).

Overall, in terms of the efficacy of the three different size of AuNPs in modulating macrophage polarization and anti-inflammation, the results above indicated that the 45 nm AuNPs showed the best performance.

3.2. AuNPs promoted the BMP-2 expression in macrophages

As previously described, macrophages can also produce BMP-2 to regulate osteogenesis. Hence, in our study, the BMP-2 expression regulated by AuNPs was assessed through real-time PCR and ELISA. As shown in Fig. 1G, in the condition without LPS stimulation, the BMP-2 mRNA level became significant higher after treatment with 45 nm AuNPs compared with the Ctrl group, while the minor upregulation of BMP-2 expression induced by 5 nm AuNPs and the down-regulatory tendency caused by 13 nm AuNPs were both not significant. However, the protein levels were not consistent, as there was little changes found when compared with Ctrl group (Fig. 1G). When LPS was present, the effects of AuNPs became much more distinct. The 45 nm AuNPs significantly promoted the mRNA expression of BMP-2 (Fig. 1H). The protein analysis indicated that the 13 nm and 45 nm AuNPs could both significantly increase the concentration of BMP-2, while the results for the 5 nm AuNPs failed (Fig. 1H).

In general, considering these findings, 45 nm AuNPs performed better in anti-inflammation and the regulation of the polarization and BMP-2 expression in macrophages. And this size-dependent regulatory effects of AuNPs on macrophages were further confirmed in murine bone marrow-derived macrophages (BMMs) and THP-1 derived macrophages. The results showed, the AuNPs with three diameters all had great biocompatibility in BMMs (Fig. S4) and could inhibit the inflammatory response aroused by LPS (Figs. S5 and S6). Among these AuNPs, the 45 nm AuNPs could downregulate the LPS-induced increased secretion of TNF-α, IL-6 and enhance the IL-10 and BMP-2 expression more effectively when compared to 5 and 13 nm AuNPs (Figs. S5 and S6). Therefore, we chose the 45 nm AuNPs for the following experiments.

3.3. In LPS activated inflammatory condition, AuNPs enhanced the osteogenic and cementogenic differentiation of hPDLCs via the interaction between AuNPs-conditioned macrophage and AuNPs-stimulated hPDLCs in the macrophage-hPDLCs coculture system

In LPS activated inflammatory condition, the effects of AuNPs on the osteogenic and cementogenic differentiation of hPDLCs in macrophage-hPDLCs coculture system through directing macrophages, hPDLCs or both cells were studied respectively through the corresponding methods shown in the schematic diagram (Figs. 2A, 3A and 4A).

First, the cell viability and proliferation in different macrophage CM were evaluated by the CCK-8 assay. The results (Fig. 2B) showed that on day 3 and day 5, four kinds of CM could all promote the growth of hPDLCs compared to that in the NC group. On day 1 and day 7, all groups had no obvious difference. Therefore, generally, the CM with or without LPS did not exert negative effects on cell proliferation.

Subsequently, the osteogenic and cementogenic differentiation of hPDLCs in different conditions was analyzed. In the noninflammatory condition, the transcription level of the osteogenic factors ALP and COL-l and cementogenic specific factor CAP in hPDLCs were all increased in the AuNPs-modulated macrophage CM (45 nm group) (Fig. 2C), though the changes in protein level was not so distinct (Fig. 2F). Similarly, the AuNPs-modulated macrophage CM also enhanced the ALP activity (Fig. 2E) and facilitated the formation of mineralized nodules in hPDLCs in the ARS and Von Kossa staining results, compared to NC group (Fig. 2G).

Meanwhile, as shown in Fig. 3, the 45 nm AuNPs could also expedited the osteogenic process with the direct use in hPDLCs in non-inflammatory macrophage CM. The mRNA expression of ALP, COL-1 and OCN (Fig. 3B), the ALP activity (Fig. 3D), and the protein levels of ALP (Fig. 3E) were increased in the AuNPs-stimulated hPDLCs (Ctrl-AuNPs group). Additionally, the ALP staining along with ARS and Von Kossa staining (Fig. 3F) also showed higher levels of ALP and calcium deposition generation with the use of AuNPs in hPDLCs. As for the specific cementogenic factors CEMP-1 and CAP, the mRNA level of CEMP-1 in Ctrl-AuNPs group was upregulated (Fig. 3B), while its protein expression and CAP expression were all not significant changed (Fig. 3E).

In the macrophage-related inflammatory microenvironment arouse by LPS (LPS group), the osteogenic differentiation of hPDLCs was inhibited, as the gene and protein expression of osteogenic factors such as Runx-2, ALP, COL-1 (Fig. 2C and F), the ALP activity (Fig. 2E) and the ALP staining (Fig. 2G) were all remarkably downregulated. What's more, no mineralization nodules was found in LPS group in the ARS and Von Kossa staining images (Fig. 2G). Interestingly, the expression of CEMP-1 and CAP measured by PCR and Western Blot was upregulated instead (Fig. 2C and F), suggesting the cementogenic differentiation was enhanced.

In such an LPS stimulated inflammatory condition, without the direct application of AuNPs in hPDLCs, the protein level of ALP and CEMP-1 (Fig. 2F) and the ALP staining (Fig. 2G) of hPDLCs in AuNPs-modulated inflammatory macrophage CM (LPS + 45 nm group) were indeed enhanced when compared with those in the LPS group. The PCR (Fig. 2C) and ALP activity (Fig. 2E) results showed that the regulatory role of AuNPs on inflammatory macrophage CM slightly increased the mRNA expression of Runx-2, ALP, COL-1, OCN, CAP and CEMP-1, though the difference with LPS group was not significant. Nevertheless, the long-term mineralized nodules formation was not ideally improved (Fig. 2G, LPS + 45 nm group).

Furthermore, the direct use of AuNPs in hPDLCs in the inflammatory microenvironment (LPS-AuNPs group) also could only slightly increased the protein levels of Runx-2, ALP and CEMP-1 compared to LPS group (Fig. 3E) and made the ALP staining became a little bit deeper (Fig. 3F). However, the direct effects of AuNPs on hPDLCs couldn't significantly inhibit the descending tendency of the Runx-2, ALP, COL-1 mRNA expression (Fig. 3B) and the ALP activity (Fig. 3D) resulting from inflammation, and the mRNA levels of CAP and CEMP-1 in LPS-AuNPs group was not further significantly increased either (Fig. 3B). The ARS staining and Von Kossa staining images showed the mineralized nodules were still nowhere to be found in the AuNPs-stimulated inflammatory hPDLCs (Fig. 3F, LPS-AuNPs group).

However, with the combination of the modulatory effects on macrophage CM and hPDLCs, the AuNPs distinctly and significantly upregulated the mRNA (Fig. 4B) and protein (Fig. 4E) levels of Runx-2, COL-1, ALP, OCN, CAP and CEMP-1. ALP activity analysis showed the same variation tendency (Fig. 4D). Similar results were also found in ALP staining as the increased ALP staining became more clear and definite with the AuNPs (Fig. 4F). Interestingly, mineralization process was accelerated with visible calcium nodules in hPDLCs with the help of AuNPs even in the inflammatory microenvironment (Fig. 4F).

What's more, the expression of the factors related to osteoclastogenesis activity including RANKL and OPG in hPDLCs was also determined. We found the mRNA expression of RANKL was increased in the inflammatory microenvironment (LPS group), while the expression of OPG was almost unchanged (Fig. 2D). The AuNPs could downregulate the expression of RANKL in hPDLCs through directing the macrophage CM (Fig. 2D). Meanwhile, the direct application of AuNPs in hPDLCs also induced the decreased expression of RANKL and

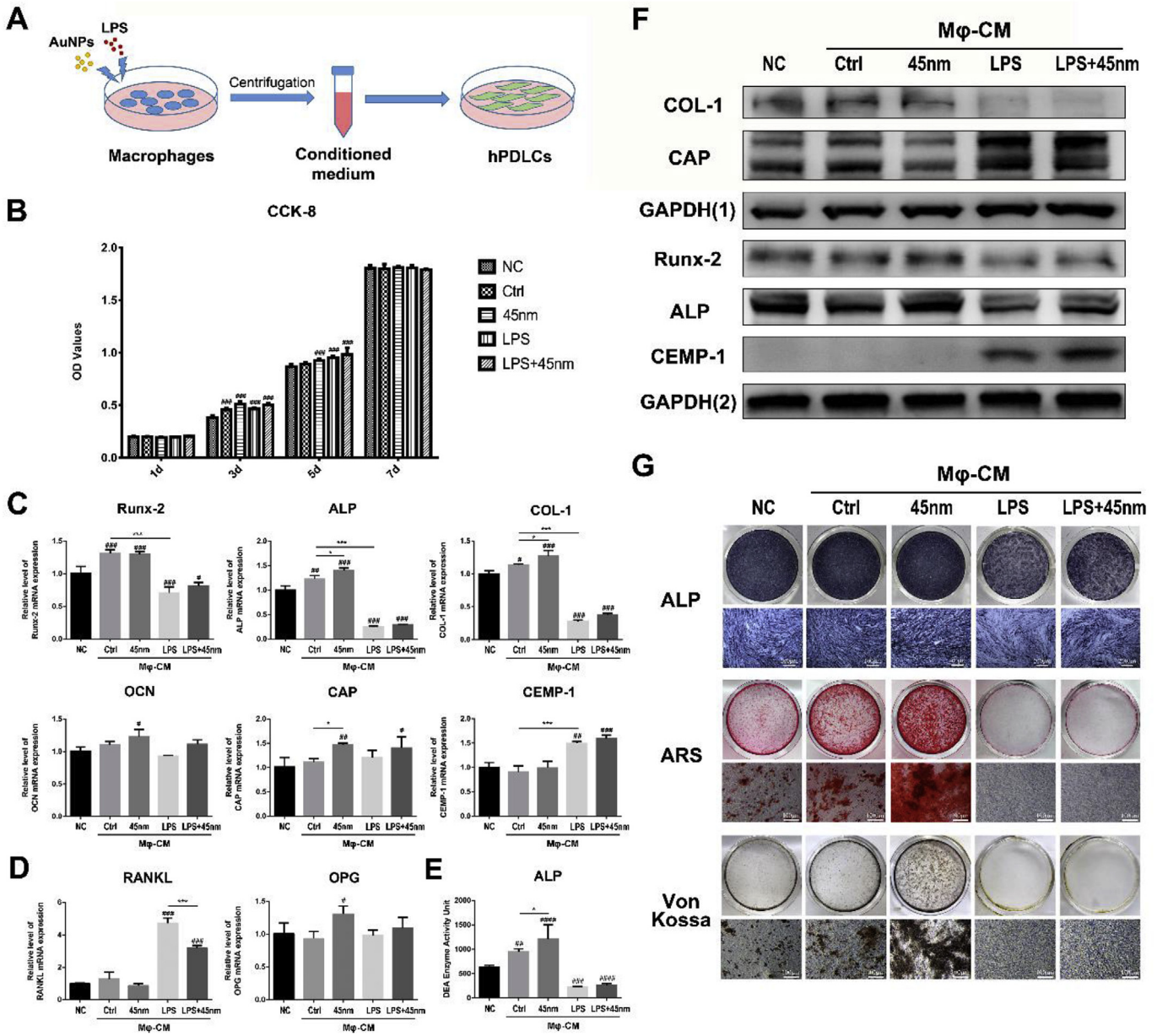

Fig. 2. AuNPs slightly promote the osteogenic and cementogenic differentiation through modulating the inflammatory macrophage CM when AuNPs are not directly applied to hPDLCs. (A) Schematic diagram of the cell processing method. (B) Cell vitality analyzed by the CCK-8 assay on day 1, day 3, day 5 and day 7. (C) Real-time PCR analysis of the relative mRNA levels of the osteogenic factors Runx-2, ALP, COL-1, and OCN and the cementogenesis-specific factors CAP and CEMP-1 on day 5. (D) Real-time PCR analysis of osteoclastic factors, including RANKL and OPG, on day 5. (E) ALP activity levels on day 7. (F) Relative protein levels of COL-1, Runx-2, ALP, CAP and CEMP-1 determined by Western blotting on day 7. (G) ALP staining on day 7 and mineralized nodules stained with ARS and Von Kossa stain on day 21. $^{\#}P < 0.05$, $^{\#\#}P < 0.01$, $^{\#\#\#}P < 0.001$, $^{\#\#\#\#}P < 0.0001$, compared with the NC group. $^{*}P < 0.05$, $^{**}P < 0.01$, $^{***}P < 0.001$. Mφ-CM = macrophage conditioned medium.

increased production of OPG (Fig. 3C). Subsequently, with the combined effects of AuNPs on the macrophages and hPDLCs, the AuNPs played an inhibitory role against the RANKL/OPG ratio change in the inflammatory microenvironment with significantly reduced mRNA level of RANKL and elevated expression of OPG (Fig. 4C).

Hence, these results indicated that, the AuNPs could effectively improve the osteogenic and cementogenic activity and downregulate the osteoclastogenesis activity through modulating the macrophage CM and hPDLCs, indicating that the AuNPs possessed great value and potential for the bone and cementum regeneration *in vitro*.

3.4. The hPDLCs in AuNPs-modulated inflammatory macrophage-hPDLCs co-culture system showed better in-vivo periodontal regeneration potential in a rat periodontal fenestration defect model

Next, to confirm the *in-vitro* enhanced osteogenic and cementogenic potential of the hPDLCs in the AuNPs-modulated inflammatory macrophage–hPDLCs coculture system and investigate the consistency between *in-vitro* and *in-vivo* studies, we used a rat periodontal fenestration defect model. As shown in the schematic diagram (Fig. 5A), the macrophage-hPDLCs system was treated with AuNPs *in vitro* and then the hPDLCs were placed into the rat periodontal defects. 3 weeks after the surgery, we observed the histological changes in the periodontal defects via H&E and Masson stained specimen sections (Fig. 5B). Based

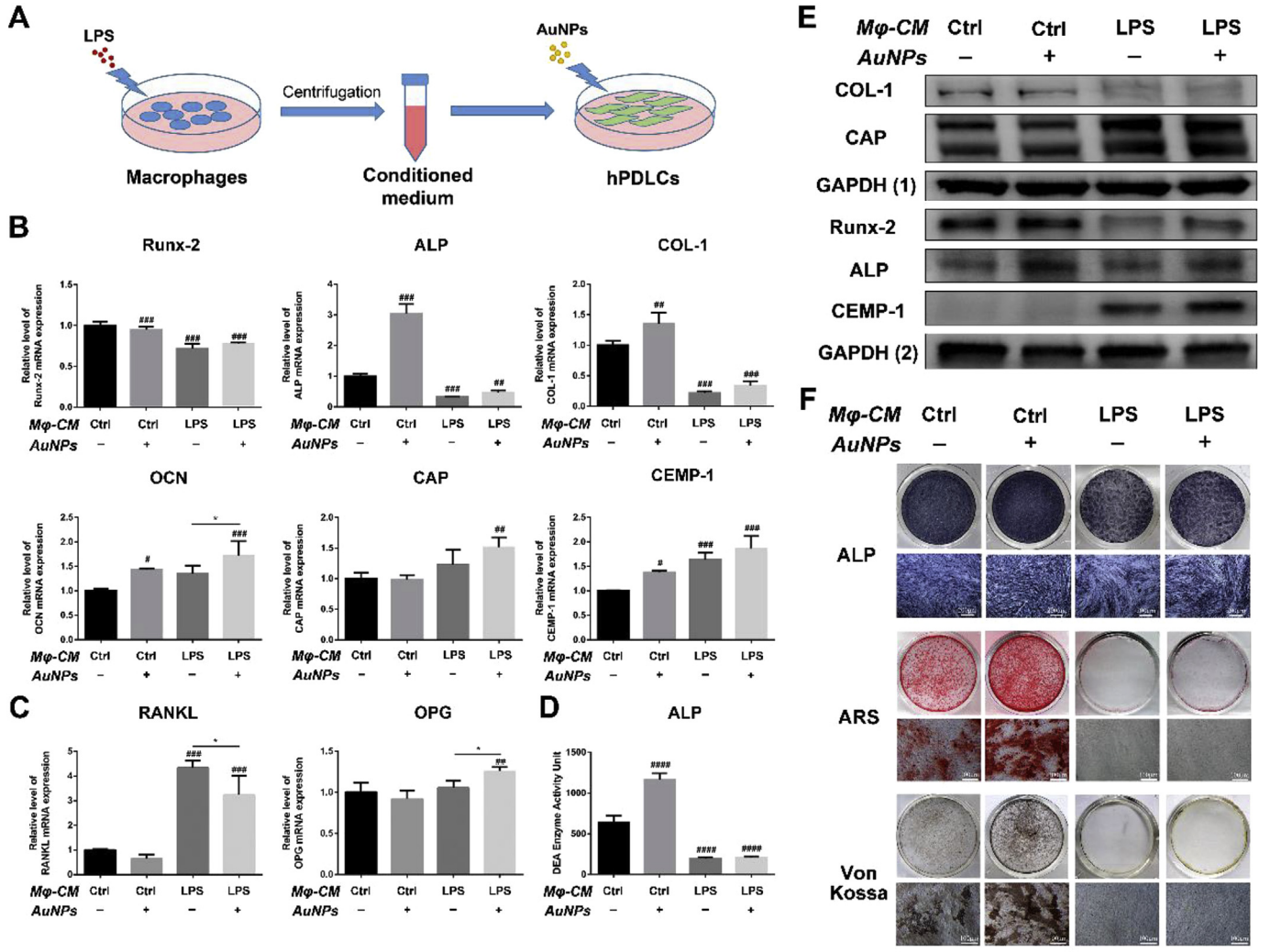

Fig. 3. In LPS-activated inflammatory condition, AuNPs slightly improve the osteogenic and cementogenic differentiation through directly modulating the hPDLCs. (A) Schematic diagram of the cell processing method. (B) Real-time PCR analysis of the relative mRNA levels of Runx-2, ALP, COL-1, OCN, CAP and CEMP-1 on day 5. (C) Real-time PCR analysis of osteoclastic factors, including RANKL and OPG, on day 5. (D) ALP activity levels on day 7. (E) Relative protein levels of COL-1, Runx-2, ALP, CAP and CEMP-1 determined by Western blotting on day 7. (F) ALP staining on day 7 and mineralized nodules stained with ARS and Von Kossa on day 21. $^{\#}P < 0.05$, $^{\#\#}P < 0.01$, $^{\#\#\#}P < 0.001$, $^{\#\#\#\#}P < 0.0001$, compared with the Ctrl group. $^{*}P < 0.05$. Mφ-CM = macrophage conditioned medium.

on the histological results, the quantity of the newly-formed tissue was calculated (Fig. 5C). Similar to the *in-vivo* results, the *in-vivo* bone regeneration potential of inflammatory hPDLCs was inhibited, as compared with Ctrl group, less newly-formed alveolar bone (NAB) was found in the periodontal defect region (LPS group). The amount of newly-formed periodontal ligament (NPDL) was also decreased in LPS group and the structure of these NPDL was sparser, more disordered and more scattered than Ctrl group. Moreover, interestingly, there was hardly any new cementum formation in the Ctrl group, but the inflammatory groups (LPS and LPS-AuNPs group) both could promote the generation of newly-formed cementum (NCem) of varying degrees, in accordance with the *in-vitro* studies. Compared with the LPS group, we observed the hPDLCs in LPS-AuNPs group with better capacity for the formation of new alveolar bone and cementum, and the NPDL in this group was also improved with thicker and denser collagen fibers, indicating that the hPDLCs in AuNPs-modulated inflammatory macrophage–hPDLCs coculture system showed better *in-vivo* regenerative potential. These results also suggest the consistency between the *in-vitro* and *in-vivo* studies about the effects of AuNPs on macrophage-hPDLCs coculture system.

3.5. AuNPs inhibited the progression of ligature-induced periodontitis in rats

In view of the effects of AuNPs on the inflammation and periodontal regeneration, an *in-vivo* study was performed to further confirm the interventional effects of AuNPs on periodontitis as shown in the schematic diagram (Fig. 6A).

Based on Micro-CT analysis, the 3D reconstructed images and different sectional images were shown in Fig. 6B. And the BMD, BV, TV, BV/TV and the bone height at six sites were also measured (Fig. 6C and D). We observed that the ligation successfully induced the periodontitis in rats and caused the bone quality loss and the bone height reduction around the teeth including the root bifurcation area (Lig group). The injection of AuNPs could remarkably alleviate the alveolar bone loss surrounding the maxillary second molars caused by ligation (Lig-AuNPs).

The H&E and Masson staining (Fig. 7A) showed that the elastic fibers and collagenous fibers were denser and more well-organized in the groups with AuNP treatment (Lig-AuNPs group), while in the Lig group, the ligature-induced periodontal inflammation led to the fiber degeneration and degradation, subsequently causing disordered and sparse arrangement of the fibers in the periodontal tissue. Furthermore, TRAP staining images (Fig. 7B) and the quantitative analysis results (Fig. 7D)

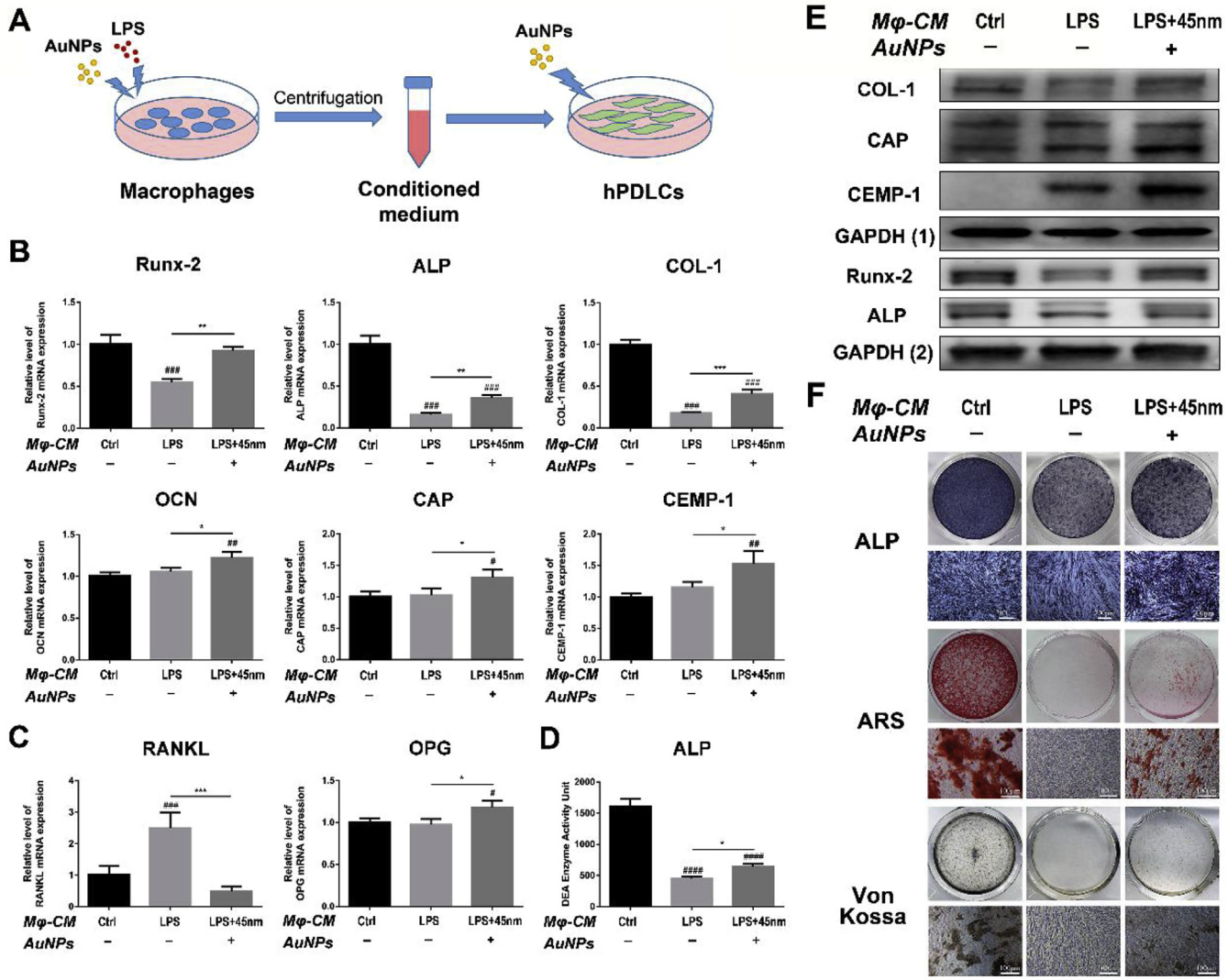

Fig. 4. In LPS-activated inflammatory condition, AuNPs significantly enhanced the osteogenic and cementogenic differentiation of hPDLCs through modulating both macrophage CM and hPDLCs. (A) Schematic diagram of the cell processing method. (B) Real-time PCR analysis of the relative mRNA levels of Runx-2, ALP, COL-1, OCN, CAP, and CEMP-1 on day 5. (C) Real-time PCR analysis of osteoclastic factors, including RANKL and OPG, on day 5. (D) ALP activity levels on day 7. (E) Relative protein levels of COL-1, Runx-2, ALP, CAP and CEMP-1 determined by Western blotting on day 7. (F) ALP staining on day 7 and mineralized nodules stained with ARS and Von Kossa on day 21. $^{\#}P < 0.05$, $^{\#\#}P < 0.01$, $^{\#\#\#}P < 0.001$, $^{\#\#\#\#}P < 0.0001$, compared with the Ctrl group. $^{*}P < 0.05$, $^{**}P < 0.01$, $^{***}P < 0.001$. Mφ-CM = macrophage conditioned medium.

showed the number of osteoclasts was decreased by AuNPs when the ligation existed. The expression of iNOS was measured by immunohistochemistry methods and the results (Fig. 7C and D) revealed that in the periodontal tissue with periodontitis, the expression of iNOS became significant higher than the Ctrl group, but the AuNPs could inhibit this inflammatory response and downregulate the level of iNOS.

4. Discussion

The periodontal tissue regeneration in periodontitis is still challenging due to the limited regenerative capacity of cementum and the adverse impact of the immune microenvironment under bacterial infection [12,35]. Recently, the crosstalk between macrophage activities and bone regeneration has been highlighted for the development and assessment of advanced biomaterials [36]. Since macrophages play crucial roles in the pathological mechanism of periodontitis, these findings provides a new strategy to investigate the potential of biomaterials in periodontal regeneration and periodontitis treatment, that is to take the activity of macrophages into consideration during the process of tissue regeneration. Moreover, since the cells with stemness like hPDLCs are the primary cells for tissue formation, the regenerative capacity of these cells is also quite essential. Thus, the macrophages and hPDLCs should be considered as an integral, and the ideal biomaterials may have the potential to regulate the immune response of macrophages and subsequently promote the tissue regeneration under this condition.

In this study, we synthesized AuNPs with different diameters including 5, 13 and 45 nm. It is known that the biophysicochemical properties like size, shape and surface hydrophobicity of the nanoparticles largely determine the nanoparticle-cell interaction. To control the surface charge and hydrodynamic size of AuNPs, stabilize the nanoparticles and induce cell penetration, AuNPs are often modified with many molecules via electrostatic, Van der Waals, coordination and hydrophobic interactions [37–40]. Cysteine is one of the common coating agents used to modify AuNPs for biomedical applications, as cysteine is a typical thiol-terminated zwitterionic biomolecule that can easily form a strong bond with the gold interface through gold-thiol chemistry [38,41,42]. The thiol group of cysteine is coordinated to the

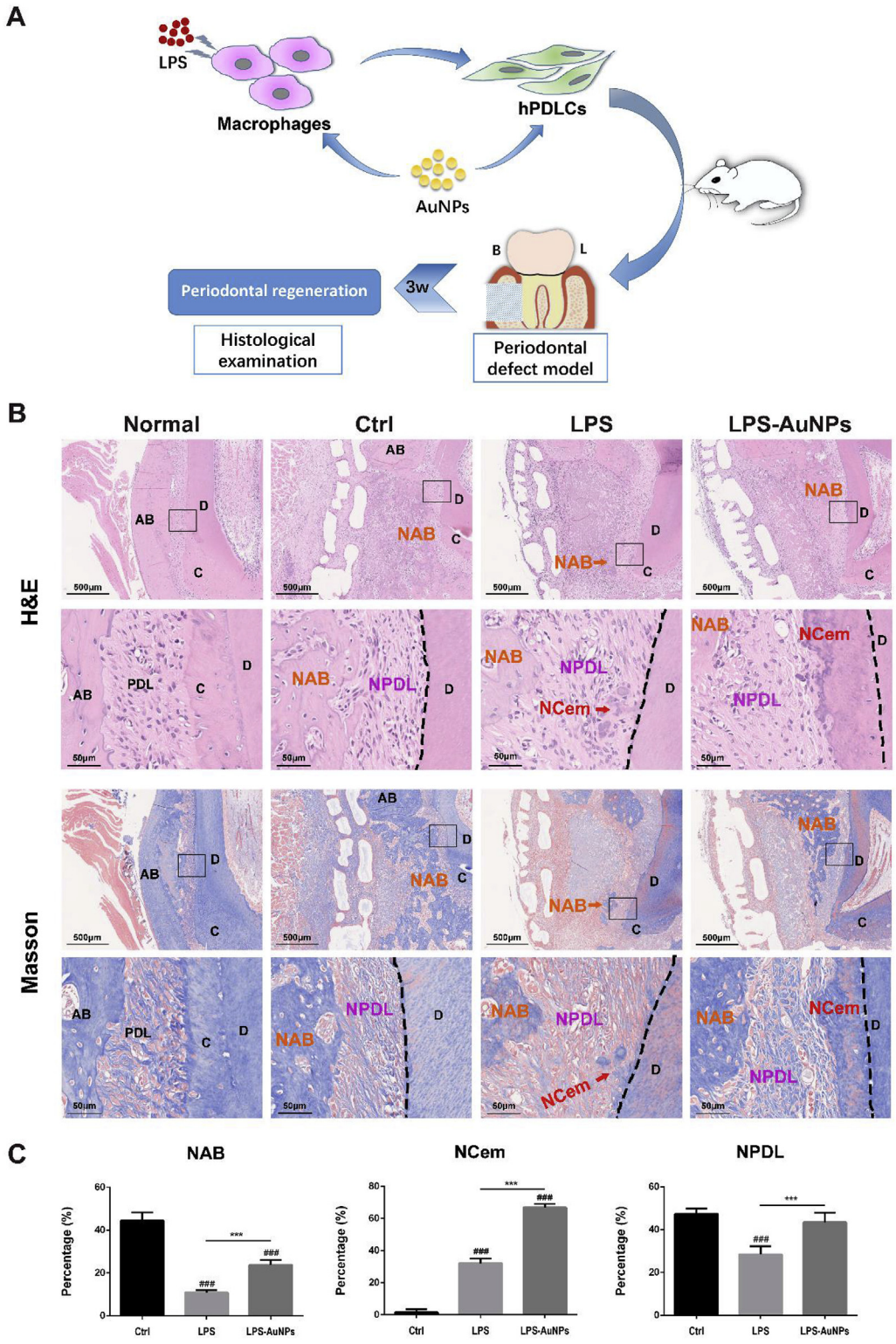

Fig. 5. The hPDLCs in AuNPs-modulated inflammatory macrophage-hPDLCs coculture system showed better in-vivo periodontal regeneration potential in a rat periodontal fenestration defect model. (A) Schematic diagram of the rat periodontal fenestration defect experiment. B = buccal side, L = Lingual side. (B) The representative H&E and Masson staining images after 3 weeks. (C) The corresponding quantitative analysis of the newly-formed alveolar bone, cementum and periodontal ligament. ###P < 0.001, compared with the Ctrl group. ***P < 0.001. AB = alveolar bone; C = cementum; D = Dentin; PDL = periodontal ligament; NPDL = newly-formed periodontal ligament; NAB = newly-formed alveolar bone; NCem = newly-formed cementum.

gold surface, whereas the deprotonated carboxy group acts as a negatively charged repulsive outer layer, so as to improve the colloidal particle stability, avoid the particle aggregation and help the cellular uptake through controlling the surface charge of the nanoparticles [42–44]. Since the cysteine is the only natural amino acid containing a thiol group, the coating with cysteine is also biocompatible and can permit the subsequent conjugation with peptides and proteins [42]. Additionally, the cysteine is also able to tailor the size, aspect ratio and optical properties of NPs and to mediate the NP assembly through the interaction of Cys zwitterions [45]. Hence the cysteine is a great coating biomolecule in the synthesis and application of AuNPs. Therefore, we used L-cysteine to cap the AuNPs. The characterization of AuNPs were measured through DLS intensities and UV–vis absorption spectra, and the results were almost the same as those of the previous study, suggesting the stability of the AuNPs [6].

The RAW 264.7 cell line has been widely used in biomedicine and biomaterial filed as a model macrophage cell line. Many studies have used the RAW 264.7 cells to study the macrophage phenotype switch,

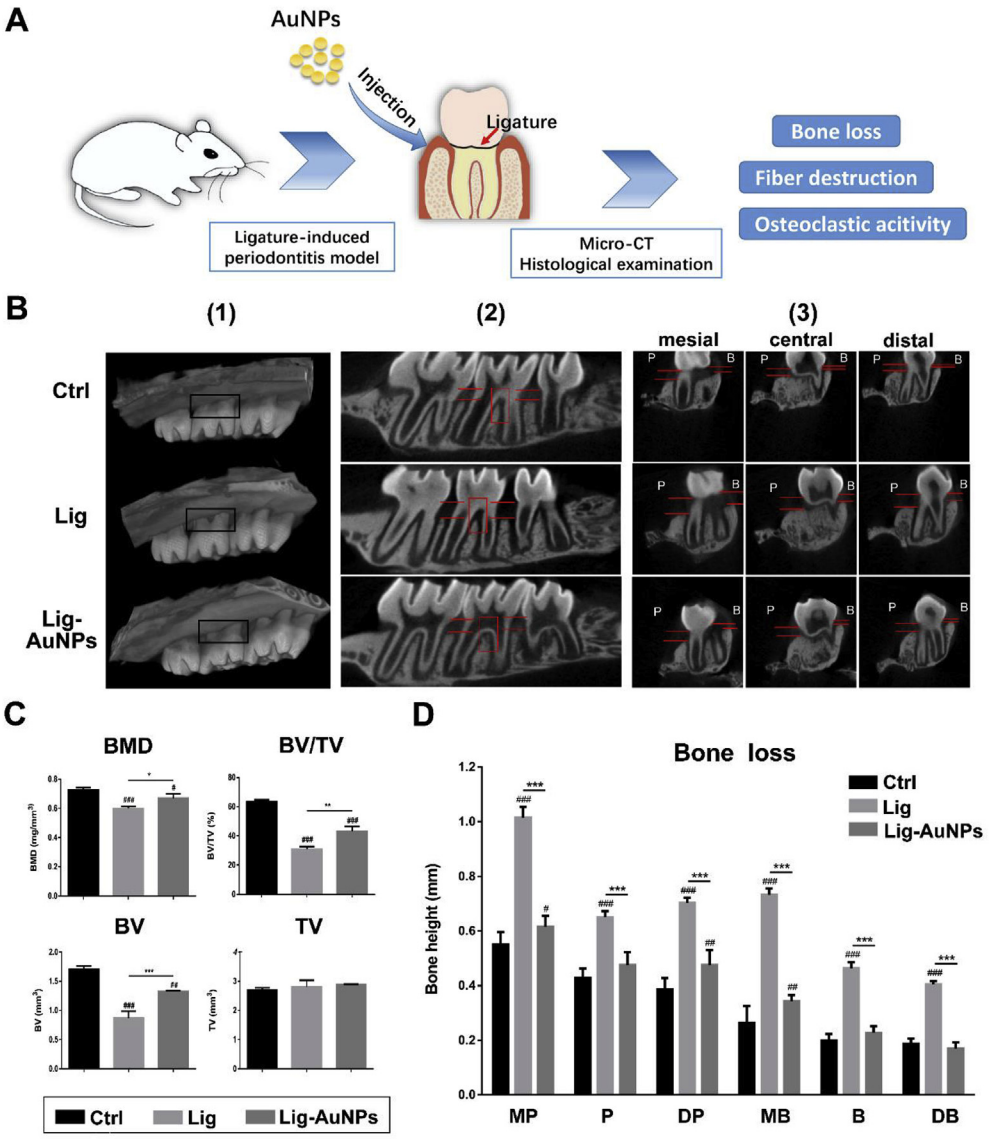

Fig. 6. AuNPs inhibited the bone loss in rat ligature-induced periodontitis. (A) Schematic diagram of the rat periodontitis experiment. (B) 3D reconstructed digitized images, mesio-distal section images and bucco-palatal section images of the maxillary second molars analyzed by Micro-CT. (C) Bone-related parameters (BMD, BV, TV and BV/TV) and (D) bone height at six sites of the maxillary second molars in different groups analyzed by Micro-CT $^{\#}P < 0.05$, $^{\#\#}P < 0.01$, $^{\#\#\#}P < 0.001$, compared with the Ctrl group. $^{*}P < 0.05$, $^{**}P < 0.01$, $^{***}P < 0.001$. MB/MP = mesial site in buccal/palatal side; B/P = central site in buccal/palatal side; DB/DP = distal site in buccal/palatal side.

inflammatory cytokine production and their influence on mesenchymal cell differentiation [21,46–48]. And the RAW 264.7 cells could most closely mimic bone marrow-derived macrophages in terms of cell phenotype surface receptors and response to microbial ligands [49]. Thus to investigate the regulatory effects of AuNPs on macrophages, we used the RAW 264.7 macrophage cells. We firstly evaluated the biocompatibility and cellular uptake of AuNPs in macrophages. The results showed AuNPs with three diameters in the concentration of 10 μM were all harmless to RAW 264.7 cells. It is reported that nanoparticles could induce a pro-oxidant environment and promote the generation of ROS in cells, thereby resulting in cell damage, apoptosis, necrosis and inflammatory response [50]. However, ROS level in our study was not enhanced by AuNPs, suggesting the great biocompatibility of AuNPs, and the result was consistent with another study [30].

Since the AuNPs are inorganic metal nanoparticles which are non-degradable, the cellular uptake and bioaccumulation of AuNPs is a meaningful and interesting issue which has raised lots of attention. The uptake of AuNPs in macrophages have been widely reported, and this process is affected by many factors including the particle size, shape and surface chemistry [51,52]. Similarly, in our study, we observed the uptake of AuNPs with three diameters in macrophages after 3 h and the internalized nanoparticles mainly located in the vesicles within cytoplasm. No AuNPs were seen in cell organelles and nucleus. Similar to other studies, the AuNP uptake into macrophages might occur through endocytosis [30,53]. Studies found that after uptake, the internalized AuNPs cells could also leave the cells through the exocytosis process [51,54,55]. Interestingly, after that, some modified AuNPs could even be re-uptaken by cells [55]. Thus the cellular accumulation of the nanoparticles might depend on the interaction between cellular uptake and exocytosis. In this study, we found the AuNPs was not absorbed completely by macrophages and the rest of the nanoparticles were remained in the culture medium after incubation with AuNPs for 24 h, as the residual AuNPs in the culture media was visible on the bottom of centrifugal tubes after centrifugation. However, to better understand the process of uptake and exocytosis and to investigate the dynamic change about the accumulation of AuNPs in macrophages, a long-term observation and much more effects may be needed in future studies.

The functional dynamic transformation of the macrophage phenotype occurs in both physiological and pathological conditions, different phenotypes play diverse role in inflammation process and tissue repair [14,56]. We observed the LPS could induce the macrophages to polarize into a pro-inflammatory M1 phenotype and increase the secretion of inflammatory factors to construct an inflammatory microenvironment. During this process, the AuNPs, especially 45 nm AuNPs, played an anti-inflammatory role through inhibiting the M1 phenotype polarization and promoting the phenotypic switch to M2 phenotype. Thus,

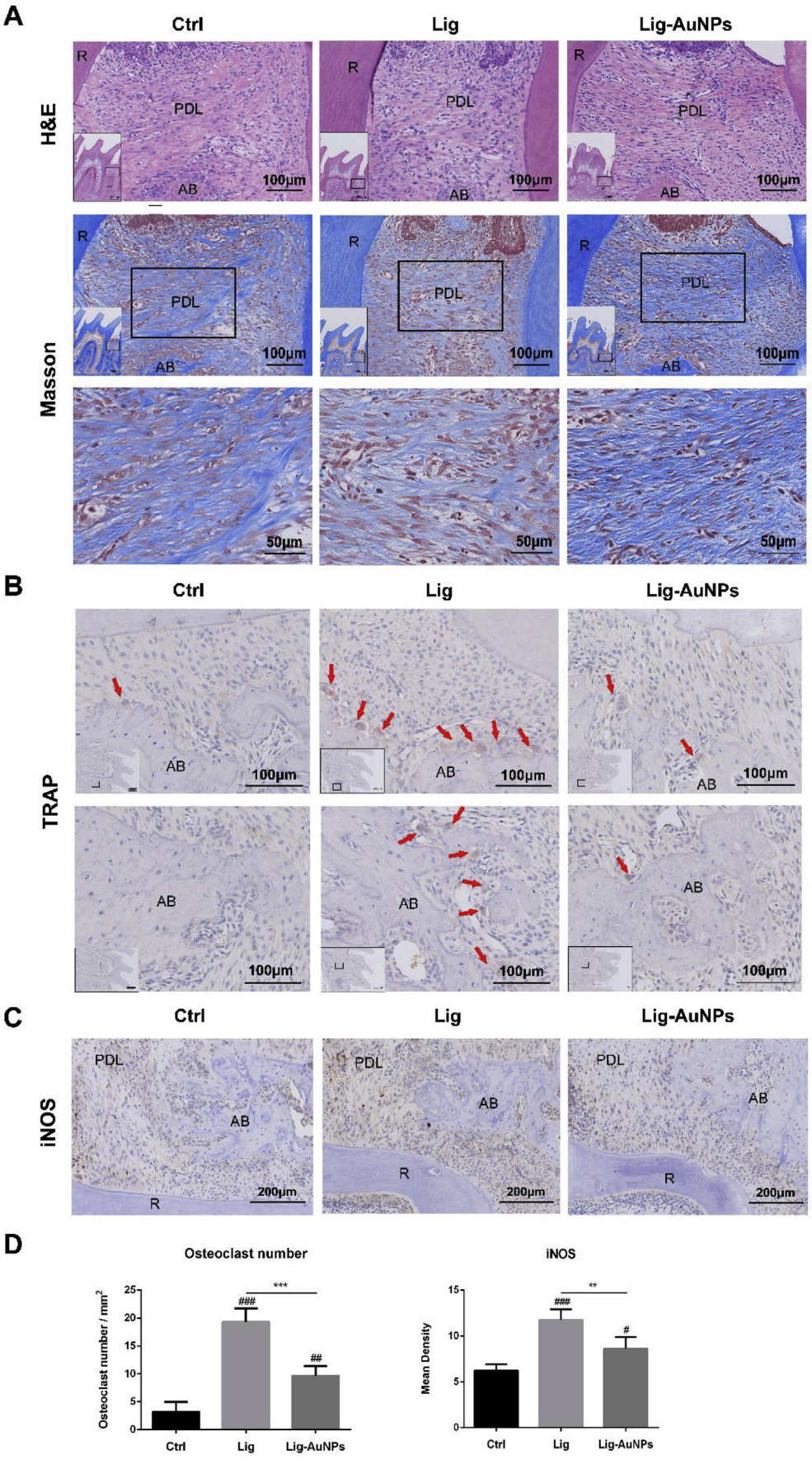

Fig. 7. AuNPs inhibited the fiber destruction, osteoclast activity and inflammatory response in rat ligature-induced periodontitis. (A) H&E and Masson staining images and (B) TRAP staining images (arrows indicate osteoblasts that are dyed red) of the maxillary second molars. (C) Expression of iNOS in the periodontal tissue of maxillary second molars analyzed using immunohistochemistry method. (D) The corresponding quantitative analysis of the osteoclast number and iNOS expression in periodontal tissues. #P < 0.05, ##P < 0.01, ###P < 0.001, compared with the Ctrl group. **P < 0.01, ***P < 0.001. AB = alveolar bone; R = root; PDL = periodontal ligament. (For interpretation of the references to colour in this figure legend, the reader is referred to the Web version of this article.)

45 nm AuNPs had great immunomodulatory effects to improve the inflammatory condition. Interestingly, at present, studies concerning the effects of AuNPs on inflammation have reached different conclusions. Some studies indicated that AuNPs can attenuate the inflammatory effects of LPS or IL-1β [29,57], while others found that AuNPs had no impact [58] or even an up-regulatory effect [59] on the inflammatory response of macrophages. The discrepancy may be caused by the differences in the surface modification, concentration and size of the AuNPs, as small changes in these features may make a big difference in the properties of AuNPs [31,32,60].

BMP-2 is an important osteogenic factor necessary for the inherent reparative capacity of bone and can accelerate the regeneration of periodontal tissues with restored structure and function [10,61]. Macrophages can also secret BMP-2 to participate in the osteogenic process [21]. However, studies focusing on BMP-2 secretion in macrophages are rare. BMP-2 belongs to the TGF-β family. It is known that TGF-β expression is associated with the M2 macrophages, however studies reported that the BMP-2 secretion in M1 and M2 macrophages was not significantly different, indicating changes in BMP-2 expression in macrophages was different from TGF-β and might be not in accordance with the macrophage polarization transformation [62]. Thus, in this study, we additionally detected the effects of AuNPs on BMP-2 secretion in macrophages and discussed it separately. We found 45 nm AuNPs showed better performance in upregulating BMP-2 expression regardless of with or without LPS stimulation, compared with 5 and 13 nm AuNPs.

Though the immortalized RAW 264.7 macrophages closely resemble the BMMs in terms of the phenotype and function, the RAW 264.7 cells might still present some diversities with the primary macrophages and macrophages from other species in their overall behavior [49]. Considering this issue, the regulatory effects of AuNPs on macrophages was further investigated in the primary BMMs and human THP-1 derived macrophages. Interestingly, the size-dependent effects of AuNPs on TNF-α, IL-6, IL-10 and BMP-2 expression were confirmed in the BMMs and THP-1 derived macrophages with great biocompatibility and similarly the 45 nm AuNPs showed better regulatory potential than 5 and 13 nm AuNPs, indicating the excellent role of AuNPs in immunomodulation.

So, 45 nm AuNPs were regarded as the optimum size as they might have better potential to generate a favorable macrophage-related immune microenvironment for tissue regeneration through regulating macrophage inflammatory response, phenotype switch and cytokines secretion. Similarly, in the earlier study of our team, the 45 nm AuNPs also showed better performance in inducing the osteogenic differentiation of hPDLCs, compared with 5 nm and 13 nm AuNPs. So based on these findings, the 45 nm AuNPs were chose for the following studies.

Considering the potential modulatory effects of AuNPs on macrophages, it was speculated that the AuNPs might be able to regulate the periodontal cell differentiation through improving the periodontal immune microenvironment. Thus the macrophages and hPDLCs were co-cultured in this study. Since the conditioned medium co-culture method has been used between cells from different species in many studies, including treating the murine cells with the conditioned media of human cells [63–65]and incubating the human cells with the conditioned media of murine cells [21,46,66,67], indicating the cells from different species can be co-cultured and the cytokines they secreted can also interact with each other, therefore, it was viable to co-culture the murine macrophages with the human primary PDLCs via the conditioned medium method. Thus the RAW 264.7 cells and hPDLCs co-culture system was established by the conditioned medium method in this study to subsequently analyze the osteogenic and cementogenic differentiation of hPDLCs in generated different macrophage CM.

We found that, in the inflammatory microenvironment, the osteogenic differentiation of hPDLCs was markedly suppressed by the inflammatory CM of macrophages stimulated by LPS. Nevertheless, another study found LPS alone does not reduce the expression of osteogenic factors or disturb the formation of calcium deposits in hPDLCs [68]. One possible reason for the variability between our studies is related to the different treatment with LPS, as in our study the LPS was used to stimulate the macrophages and subsequently the CM of macrophages was collected to treat hPDLCs, while in another study the LPS was used directly on hPDLCs. LPS, an important structural component of the outer membrane of gram-negative bacteria, can lead to an inflammatory response after recognition by Toll-like receptor 4 (TLR4) [69,70]. Since immune cells, such as macrophages and monocytes, mainly express TLR4 and are crucial members in the innate immune response, these cells are more susceptible to LPS than other nonimmune cells, like hPDLCs [71]. This susceptibility is proved from another point of view: when cells are stimulated with *E. coli* LPS, the expression of TLR4 which corresponds to the magnitude of the LPS response is up-regulated in monocytes but does not significantly change in osteoblasts [72,73]. Therefore, it is reasonable to speculate that macrophages are the main target cells of LPS and are responsible for most of the actions of LPS. Accordingly, in our study, although the CM might contain residual LPS, the inhibition effect on osteogenesis may result from the cytokines in the CM produced by macrophage cells rather than from LPS itself. Consistent with our inference, an *in vivo* study demonstrated that the inhibition of osteogenesis induced by LPS in a murine model is dependent on TNF-α [74]. Moreover, similar results showing that TNF-α, IL-1β and IL-6 can suppress osteogenesis were reported *in vitro* [75–79]. In the same way, our study has demonstrated that the CM of the macrophages treated with LPS group contained more TNF-α and IL-6 than the media of the other groups, consequently leading to decreased osteogenic activity. Hence, it is noted that it's not sufficient to simply use LPS in osteoblasts and stem cells to simulate the inflammatory condition *in vitro*, as the inflammatory microenvironment should be mainly constructed by immune cells instead.

Cementum is a vital component in periodontal tissues, however, opposite to osteogenic proteins, the expression of specific cementum proteins including CAP and CEMP-1 were both enhanced in the inflammatory microenvironment. It is really interesting as some studies has reported that TNF-α had a negative impact on cementoblast differentiation [8,80], but in our study, the inflammatory CM with increased TNF-α promoted the cementogenic differentiation. There are some discrepancies between these results and ours case: first of all, the cells are different, other studies used the OCCM-30 immortalized cementoblast cell line, we used the hPDLCs; second, the CM contains various cytokines, including inflammatory and anti-inflammatory factors, osteogenic factors, and fibrogenic factors, that is, the microenvironment constructed by the CM was much more complicated than that with TNF-α alone; hence, these elements may be responsible for the differences in the results. In addition, concerning the contrary effect on bone and the cementum system, the Wnt signaling pathway may participate in the process. The weakening of the bone-regeneration ability of periodontal ligament stem cells (PDLSCs) induced by an inflammatory microenvironment with TNF-α and IL-1β was found to arise from the increased level of β-catenin [79]. In contrast, the activation of the Wnt/β-catenin signaling pathway has been proved to promote cementum regeneration both *in vivo* and *in vitro* [7,35]. Thus, the processes of bone regeneration and cementum formation may be not synchronous as the two process react differently to the Wnt/β-catenin signaling pathway.

Another finding was that in non-inflammatory condition, the CM regulated by AuNPs on macrophages promoted the osteogenic differentiation of hPLDCs. However, in the inflammatory condition, even though the immune microenvironment modulated by 45 nm AuNPs was comprised with lower concentrations of TNF-α and IL-6 and higher BMP-2 and IL-10 expression in macrophages cultured with LPS, the generated microenvironment only facilitated the osteogenic and cementogenic activity to some extent and failed to improve the long-term mineralization result. These results revealed that immunoregulatory

effects of AuNPs did play a role on the osteogenesis and cementogenesis in a short term. However, under the chronic inflammatory microenvironment for a long-term, the stimulation of the residual inflammatory factors also disrupted the function of hPDLCs and downregulated their regenerative potential. So in the macrophage-hPDLCs coculture system, only focusing on the modulatory role of AuNPs on macrophages to improve the inflammatory microenvironment might not be enough to reverse the long-term outcome.

Then we investigate the individual effects of AuNPs on hPDLCs without considering the regulation of macrophage CM. The CM of macrophage cells treated without or with LPS was used to simulate the non-inflammatory or inflammatory microenvironment. Interestingly, in the noninflammatory condition, the 45 nm AuNPs expedited the osteogenic differentiation, consistent with other studies [6,81–83]. However, in the inflammatory microenvironment, the role of AuNPs in osteogenesis was weaken a lot. Merely relying on the direct effects of AuNPs on hPDLCs was still not enough to significantly enhance the osteogenic and cementogenic activity and improve the long-term calcification formation of hPDLCs in a microenvironment with a strong inflammatory response. These findings also confirmed the importance of immune cells in tissue regeneration. It is noted that the modulation of the macrophage-related immune microenvironment is quite essential in regulating periodontal cell differentiation, since an unfavorable immune microenvironment is detrimental to successful bone and cementum regeneration and can affect the performance of biomaterials.

Since the AuNPs could play a role on osteogenesis and cementogenesis through regulating macrophages and hPDLCs, it is needful to combine these two interrelated and indispensable effects together when assessing the effects of AuNPs on periodontal regeneration *in vitro*. Interestingly, with the interaction between AuNPs-conditioned macrophages and AuNPs-stimulated hPDLCs, AuNPs significantly upregulated the osteogenic and cementogenic differentiation of hPDLCs and accelerated the mineralization process in the inflammatory microenvironment.

What's more, the bone regeneration process is inseparable with osteoclast activity. Since the dynamic equilibrium of bone tissue may be attributed to the regulation of RANK-RANKL-OPG axis and the hPDLCs can also express RANKL and OPG, thus the RANKL/OPG expression ratio in hPDLCs was measured [12,84–86]. It is well known that increasing RANKL/OPG ratio can result in bone resorption; otherwise, bone formation will take place. We observed that in the inflammatory microenvironment, the RANKL/OPG ratio increased, suggesting more osteoclastogenesis activity. However, with the immunoregulatory effects of AuNPs on macrophages, the level of RANKL was decreased in AuNPs-modulated inflammatory macrophage CM, thus depressing the osteoclast process with lower RANKL/OPG ratio. The changes about RANKL/OPG expression conformed to the findings in osteoimmunology that the inflammatory cytokines, such as TNF-α, IL-6 and IL-1, can enhance the RANKL/OPG ratio, while anti-inflammatory factors, such as IL-4 and IL-10, play the opposite role [12,85]. The AuNPs downregulated the TNF-α and IL-6 expression, and increased the IL-10 secretion in the macrophages CM, giving AuNPs the possible ability to decrease the RANKL/OPG ratio. In addition, the direct application of AuNPs in hPDLCs could also bring some internal change to the cells, subsequently inhibited the upregulation of RANKL/OPG ratio caused by inflammation. As the AuNPs could regulate the RANKL/OPG expression in these two ways, AuNPs might have great potential in inhibiting osteoclast activity and bone loss. Therefore, it revealed that AuNPs might be a possible therapeutic agent for osteoclast-related bone metabolism diseases, including periodontitis.

In this study, the AuNPs affected the function of both macrophages and hPDLCs and the issues about how they worked were quite interesting. Nowadays, the mechanisms under these AuNPs-induced cellular functional changes have aroused wide concerns. In macrophages, various signaling pathway have been found to be involved with the anti-inflammatory effects of AuNPs in macrophages, such as tuberin-mTOR/NF-κB pathways [87], p38 MAPK/NF-κB and Ap-1 pathways [88,89]. Studies also found AuNPs could regulate the osteogenic differentiation of osteoblasts and stem cells including the hPDLCs through P38 MAPK pathway [81,90], ERK/MAPK signaling pathway [91], Wnt/β-catenin signaling pathway [82] and autophagy [6]. Moreover, AuNPs also play a role in the differentiation, viability and cellular behaviors of other cells through mTOR/p70S6K pathway [92], Akt pathway [93] as well as autophagy and apoptosis [93–95]. So the effects of AuNPs involve multi-pathways and the relationship between these pathways and the participation of other possible mechanisms may need further investigation in the future.

Above all, the *in vitro* studies suggested the 45 nm AuNPs promoted the osteogenesis and cementogenesis process and downregulated the osteoclastogenesis activity through modulating the macrophage-hPDLCs co-culture system, thus AuNPs might have great potential for periodontal regeneration. This finding was further confirmed in a rat periodontal fenestration defect model. This animal model is a traditional model for the observation of periodontal tissues regeneration through constructing a mandibular critical-size defect of bone, cementum and periodontal ligament and has been used for decades [7,34]. In the *in-vivo* study, we could find that the hPDLCs in the AuNPs-modulated inflammatory macrophage-hPDLCs co-culture system did have better performance in *in-vivo* bone, cementum regeneration after implanted into the defect area when compared to the those inflammatory cells without AuNPs modulation, which was in accordance with the *in-vitro* results. The collagen fiber regeneration was also enhanced after treated with AuNPs. *In vitro* study showed that the AuNPs could increase the expression of TGF-β in macrophages in the inflammatory condition. As the TGF-β is generally considered a fibrogenic factor and may promoted the hPDLCs to form collagen fibers, the *in-vivo* changes in fibers agreed with the TGF-β expression, proving the essential role of macrophages in periodontal regeneration and the biological function of biomaterials once again.

Thus, the AuNPs could inhibit the inflammation and promote the periodontal regeneration, so they might be a promising option for periodontitis treatment. This conjecture is followed by an *in-vivo* studies in s ligature-induced periodontitis model to confirm the therapeutic values of AuNPs in periodontitis. The ligature method is considered a well-acknowledged traditional way to simulate periodontitis and has been used in many relevant studies [96–98]. This model is reported to be similar to human periodontitis in various aspects, as the alveolar bone resorption depends on bacteria and gingival tissue is infiltrated with inflammatory cells [99]. It is well known that the inflammation and bone loss sustained throughout the ligation period mainly depends on the ligature-induced accumulation of bacteria in the ligature placement site, thus the ligature-induced model is suitable for the investigation of host response and periodontal tissue loss and repair [100]. In the previous studies of our team, the periodontitis model was successfully established in mice by ligation [101]. The intervention of AuNPs in the animal models prevent the progression of bone loss and fiber destruction. Moreover, the osteoclast activity was also weakened by AuNPs in periodontitis models, in accordance with the *in-vitro* study about the RANK/OPG expression. Corresponding to the Micro-CT and *in-vitro* results, inflammation promoted the generation and activity of osteoclasts and decreased the osteogenic activity, consequently damaging the bone tissue, whereas the AuNPs suppressed this pathological process and decreased the bone loss. These findings verified the consistency between the *in-vitro* study and the *in-vivo* study and provided strong evidence for the therapeutic potential of AuNPs for treating periodontitis. What's more, the expression of iNOS in the periodontal tissue treated with AuNPs was also downregulated, which indicated the relief of the inflammation. iNOS was expressed by M1 phenotype macrophages. The *in-vitro* study had shown the AuNPs inhibited the M1 polarization of macrophages caused by LPS and decreased the iNOS expression, and this result was accordant with the *in-vivo* iNOS expression in the animal experiments. These consistencies found between

in-vitro and *in-vivo* studies suggested the necessity and veracity of taking the macrophages and hPLDCs as a whole in the *in-vitro* studies about periodontal regeneration.

Currently, the distribution and bioaccumulation of AuNPs *in vivo* is also a crucial issue and much progress have been made in this field. Many studies have found that after intravenous administration with AuNPs, the AuNPs could be distributed to many organs like liver, kidney, lung, spleen, intestine et al., and the particle size and surface charge strongly determine the unequal accumulation of AUNPs in these tissues [102–105]. Excretion of gold in feces and urine could also be observed and the clearance of AuNPs *in vivo* is mainly through the hepatobiliary system into fecal excretion [103–106]. In this study, after injection with AuNPs for 4 h, we have used ICP-MS to determine amount of the AuNPs in the gingival tissue, and the results showed 0.33 mg/L of the AuNPs in the gingival tissue homogenate, indicating the AuNPs have been absorbed by the gingival tissues. On the basis of those previous findings, we could speculate that the AuNPs injected to the gingival tissue might subsequently translocate into blood and distribute into other tissues through the blood circulation, finally excrete into feces. To figure out the distribution and clearance of AuNPs in this *in-vivo* study and to verify this conjecture, a long-time observation about the accumulation and excretion of AuNPs will be needed in the further studies.

In general, this study found AuNPs modulated the crosstalk between macrophages and hPDLCs for periodontal regeneration and periodontitis treatment. Actually, the process of periodontal tissue destruction and regeneration is quite complex with the involvement of lots of cells. In the pathogenesis of periodontitis, the inflammatory condition and tissue damage is associated with the host immune response provoked by the invading bacteria [11]. This process involves a variety of immune cells, including macrophages, T cells, B cells, polymorphonuclear neutrophils (PMN) et al., and the modulation of these cells might be a potential therapeutic target for periodontitis treatment [11,14,15,107–109]. The macrophages are the major source of the destructive factors like TNF-α, IL-1, IL-6 in the periodontal inflammatory microenvironment and are crucial contributors to tissue breakdown [11,13,15]. Thus we choose the macrophages as one of the objects of this study. However, the activity of many other immune cells also contribute to the tissue loss. In the infectious condition of periodontitis, the macrophages also present antigens to T cells to activate the T cells and adaptive immunity [11]. The T cells are classified into many subpopulations which play diverse roles [108]. The $CD4^+$ T cells are the major T cells responsible for the T-cell immune responses against pathogens and they includes the T-helper 1 cells (Th1), T-helper 2 cells (Th2) and T-helper 17 cells (Th17) [11]. The Th1, Th17 cells are reported to be associated the tissue loss through the expression of RANKL and inflammatory cytokines, while Th2 cells could protect the periodontal tissues from destruction [11,108]. Interestingly, the T-helper cells (Th1/Th2 cells) can also affect the macrophage polarization, as Th1 cells produce large quantities of IFN-γ, activate macrophages to M1 phenotype and are essential for the defense against intracellular pathogens, while Th2 cells mainly produce IL-4 to activate macrophages to M2 phenotype and mediate recruitment of eosinophils to sites of inflammation to help clear parasitic infections [11,14]. Similar to T cells, the activated B cells can also contribute to the increased periodontal bone resorption through secreting RANKL [11,108]. Furthermore, in the periodontal tissue, the PMNs infiltration acts like a double-edged sword, as they not only eliminate the invasion of microorganism, but also can further damage the tissue [107]. The hyperactive activity of PMNs and excessive PMN degranulation in periodontitis are thought to be engaged in the tissue destruction [11,107]. Above all, these immune cells collaborate with each other and generate a periodontal inflammatory microenvironment with plenty of inflammatory cytokines and osteoclastogenesis related factor RANKL in periodontitis, subsequently influence the regenerative potential of the periodontal cells and enhance the osteoclast activity. Therefore, the interaction between the immune cells, the periodontal cells with differentiation capacity and the osteoclasts are responsible for the periodontal tissue loss. Considering the participation of so many cells in periodontitis, the crosstalk between these cells is quite necessary and valuable to investigate in periodontitis, which also provided a proper strategy for periodontitis treatment. In this study, we mainly focus on the macrophages and hPDLCs, and the possible crosstalk between other types of cells still need further studies.

5. Conclusions

In summary, this study, for the first time, investigated the application of AuNPs in periodontal regeneration in terms of the crosstalk between macrophages and hPDLCs. We demonstrated that the 45 nm AuNPs could regulate favorable inflammatory response, macrophage polarization and cytokines production of macrophages, thus improve the inflammatory microenvironment for periodontal tissue regeneration. These findings suggested that AuNPs might be a potential therapeutic option in periodontal tissue engineering and periodontitis therapy.

Data availability

The authors declare that all data supporting the findings of this study are available within the paper and Supplementary Information.

Conflicts of interest

The authors have no conflicts of interest to declare.

Author contributions

Can Ni and Fuhua Yan designed the study and improved the research plan with the guidance of Yin Xiao and Wenrong Yang. Na Kong and Wenrong Yang synthesized the AuNPs. Can Ni did the *in vitro* experiments and the *in vivo* experiment on the rat periodontal fenestration defect models with the assistance of Tianying Bian and Yangheng Zhang. Jing Zhou performed the study about the intervention of AuNPs on a rat ligature-induced periodontitis and contributed to the data analyses in this experiment. Xiaofeng Huang assisted in the histological analysis of the tissue sections. Can Ni was responsible for the data analyses and wrote the manuscript. Yin Xiao, Wenrong Yang and Fuhua Yan were involved in the revision of the manuscript.

Acknowledgements

This study was financially supported by the National Natural Science Foundation Project (No. 81570982, 81771078) and the Project of Invigorating Health Care through Science, Technology and Education (No. CXTDB2017014). The authors thank Central Laboratory of Stomatology, Nanjing Stomatological Hospital, Medical School of Nanjing University.

Appendix A. Supplementary data

Supplementary data to this article can be found online at https://doi.org/10.1016/j.biomaterials.2019.03.039.

References

[1] G. Hajishengallis, Periodontitis: from microbial immune subversion to systemic inflammation, Nat. Rev. Immunol. 15 (1) (2015) 30–44.
[2] R.P. Darveau, Periodontitis: a polymicrobial disruption of host homeostasis, Nat. Rev. Microbiol. 8 (7) (2010) 481–490.
[3] Y. Yu, C.S. Bi, R.X. Wu, Y. Yin, X.Y. Zhang, P.H. Lan, F.M. Chen, Effects of short-term inflammatory and/or hypoxic pretreatments on periodontal ligament stem cells: in vitro and in vivo studies, Cell Tissue Res. 366 (2) (2016) 311–328.

[4] S.I. Lee, D.W. Lee, H.M. Yun, H.J. Cha, C.H. Bae, E.S. Cho, E.C. Kim, Expression of thymosin beta-4 in human periodontal ligament cells and mouse periodontal tissue and its role in osteoblastic/cementoblastic differentiation, Differentiation 90 (1–3) (2015) 16–26.

[5] J. Nuñez, S. Sanz-Blasco, F. Vignoletti, F. Muñoz, R.G. Caffesse, M. Sanz, C. Villalobos, L. Nuñez, 17β-Estradiol promotes cementoblast proliferation and cementum formation in experimental periodontitis, J. Periodontol. 81 (7) (2010) 1064–1074.

[6] Y. Zhang, N. Kong, Y. Zhang, W. Yang, F. Yan, Size-dependent effects of gold nanoparticles on osteogenic differentiation of human periodontal ligament progenitor cells, Theranostics 7 (5) (2017) 1214–1224.

[7] P. Han, S. Ivanovski, R. Crawford, Y. Xiao, Activation of the canonical Wnt signaling pathway induces cementum regeneration, J. Bone Miner. Res. 30 (7) (2015) 1160–1174.

[8] X. Wang, H. Sun, H. Liao, C. Wang, C. Jiang, Y. Zhang, Z. Cao, MicroRNA-155-3p mediates TNF-alpha-inhibited cementoblast differentiation, J. Dent. Res. 96 (12) (2017) 1430–1437.

[9] S. Li, J. Shao, Y. Zhou, T. Friis, J. Yao, B. Shi, Y. Xiao, The impact of Wnt signalling and hypoxia on osteogenic and cementogenic differentiation in human periodontal ligament cells, Mol. Med. Rep. 14 (6) (2016) 4975–4982.

[10] F.-M. Chen, R.M. Shelton, Y. Jin, I.L.C. Chapple, Localized delivery of growth factors for periodontal tissue regeneration: role, strategies, and perspectives, Med. Res. Rev. 29 (3) (2009) 472–513.

[11] R.A. Kayal, The role of osteoimmunology in periodontal disease, BioMed Res. Int. 2013 (2013) 1–12.

[12] D.L. Cochran, Inflammation and bone loss in periodontal disease, J. Periodontol. 79 (8s) (2008) 1569–1576.

[13] T. Yu, L. Zhao, X. Huang, C. Ma, Y. Wang, J. Zhang, D. Xuan, Enhanced activity of the macrophage M1/M2 phenotypes and phenotypic switch to M1 in periodontal infection, J. Periodontol. 87 (9) (2016) 1092–1102.

[14] C. Sima, M. Glogauer, Macrophage subsets and osteoimmunology: tuning of the immunological recognition and effector systems that maintain alveolar bone, Periodontolgy 63 (1) (2000) 80–101 (2013).

[15] Z. Zhuang, S. Yoshizawa-Smith, A. Glowacki, K. Maltos, C. Pacheco, M. Shehabeldin, M. Mulkeen, N. Myers, R. Chong, K. Verdelis, G.P. Garlet, S. Little, C. Sfeir, Induction of M2 macrophages prevents bone loss in murine periodontitis models, J. Dent. Res. 98 (2) (2019) 200–208.

[16] D. Zhou, C. Huang, Z. Lin, S. Zhan, L. Kong, C. Fang, J. Li, Macrophage polarization and function with emphasis on the evolving roles of coordinated regulation of cellular signaling pathways, Cell. Signal. 26 (2) (2014) 192–197.

[17] L.B. Ivashkiv, Epigenetic regulation of macrophage polarization and function, Trends Immunol. 34 (5) (2013) 216–223.

[18] A. Mantovani, A. Sica, S. Sozzani, P. Allavena, A. Vecchi, M. Locati, The chemokine system in diverse forms of macrophage activation and polarization, Trends Immunol. 25 (12) (2004) 677–686.

[19] S. Gordon, F.O. Martinez, Alternative activation of macrophages: mechanism and functions, Immunity 32 (5) (2010) 593–604.

[20] P.A. Muller, B. Koscso, G.M. Rajani, K. Stevanovic, M.L. Berres, D. Hashimoto, A. Mortha, M. Leboeuf, X.M. Li, D. Mucida, E.R. Stanley, S. Dahan, K.G. Margolis, M.D. Gershon, M. Merad, M. Bogunovic, Crosstalk between muscularis macrophages and enteric neurons regulates gastrointestinal motility, Cell 158 (2) (2014) 300–313.

[21] Z. Chen, C. Wu, W. Gu, T. Klein, R. Crawford, Y. Xiao, Osteogenic differentiation of bone marrow MSCs by beta-tricalcium phosphate stimulating macrophages via BMP2 signalling pathway, Biomaterials 35 (5) (2014) 1507–1518.

[22] K. Nagatomo, M. Komaki, I. Sekiya, Y. Sakaguchi, K. Noguchi, S. Oda, T. Muneta, I. Ishikawa, Stem cell properties of human periodontal ligament cells, J. Periodontal. Res. 41 (4) (2006) 303–310.

[23] B.-M. Seo, M. Miura, S. Gronthos, P. Mark Bartold, S. Batouli, J. Brahim, M. Young, P. Gehron Robey, C.Y. Wang, S. Shi, Investigation of multipotent postnatal stem cells from human periodontal ligament, Lancet 364 (9429) (2004) 149–155.

[24] D. Cabuzu, A. Cirja, R. Puiu, A.M. Grumezescu, Biomedical applications of gold nanoparticles, Curr. Top. Med. Chem. 15 (16) (2015) 1605–1613.

[25] Z. Liu, Y. Shen, Y. Wu, Y. Yangg, J. Wu, P. Zhou, X. Lu, Z. Guo, An intrinsic therapy of gold nanoparticles in focal cerebral ischemia-reperfusion injury in rats, J. Biomed. Nanotechnol. 9 (6) (2013) 1017–1028.

[26] K. Tyner, S. Bancos, D. Stevens, Effect of silica and gold nanoparticles on macrophage proliferation, activation markers, cytokine production, and phagocytosis in vitro, Int. J. Nanomed. (2014) 183.

[27] N. Lewinski, V. Colvin, R. Drezek, Cytotoxicity of nanoparticles, Small 4 (1) (2008) 26–49.

[28] M. Kingston, J.C. Pfau, J. Gilmer, R. Brey, Selective inhibitory effects of 50-nm gold nanoparticles on mouse macrophage and spleen cells, J. Immunotoxicol. 13 (2) (2016) 198–208.

[29] V.V. Sumbayev, I.M. Yasinska, C.P. Garcia, D. Gilliland, G.S. Lall, B.F. Gibbs, D.R. Bonsall, L. Varani, F. Rossi, L. Calzolai, Gold nanoparticles downregulate interleukin-1beta-induced pro-inflammatory responses, Small 9 (3) (2013) 472–477.

[30] Q. Zhang, V.M. Hitchins, A.M. Schrand, S.M. Hussain, P.L. Goering, Uptake of gold nanoparticles in murine macrophage cells without cytotoxicity or production of pro-inflammatory mediators, Nanotoxicology 5 (3) (2011) 284–295.

[31] X. Chen, C. Gao, Influences of size and surface coating of gold nanoparticles on inflammatory activation of macrophages, Colloids Surfaces B Biointerfaces 160 (2017) 372–380.

[32] H.-J. Yen, S.-H. Hsu, C.-L. Tsai, Cytotoxicity and immunological response of gold and silver nanoparticles of different sizes, Small 5 (13) (2009) 1553–1561.

[33] Y. Zhang, J. Liu, D. Li, X. Dai, F. Yan, X.A. Conlan, R. Zhou, C.J. Barrow, J. He, X. Wang, W. Yang, Self-assembled core-satellite gold nanoparticle networks for ultrasensitive detection of chiral molecules by recognition tunneling current, ACS Nano 10 (5) (2016) 5096–5103.

[34] C. Chen, H. Li, J. Jiang, Q. Zhang, F. Yan, Inhibiting PHD2 in bone marrow mesenchymal stem cells via lentiviral vector-mediated RNA interference facilitates the repair of periodontal tissue defects in SD rats, Oncotarget (2017) 72676–72699.

[35] P. Han, C. Wu, J. Chang, Y. Xiao, The cementogenic differentiation of periodontal ligament cells via the activation of Wnt/beta-catenin signalling pathway by Li+ ions released from bioactive scaffolds, Biomaterials 33 (27) (2012) 6370–6379.

[36] Z. Chen, T. Klein, R.Z. Murray, R. Crawford, J. Chang, C. Wu, Y. Xiao, Osteoimmunomodulation for the development of advanced bone biomaterials, Mater. Today 19 (6) (2016) 304–321.

[37] J.A. Salazar-González, O. González-Ortega, S. Rosales-Mendoza, Gold nanoparticles and vaccine development, Expert Rev. Vaccines 14 (9) (2015) 1197–1211.

[38] S. Monti, V. Carravetta, H. Agren, Decoration of gold nanoparticles with cysteine in solution: reactive molecular dynamics simulations, Nanoscale 8 (26) (2016) 12929–12938.

[39] D. An, J. Su, J.K. Weber, X. Gao, R. Zhou, J. Li, A peptide-coated gold nanocluster exhibits unique behavior in protein activity inhibition, J. Am. Chem. Soc. 137 (26) (2015) 8412–8418.

[40] A.E. Nel, L. Madler, D. Velegol, T. Xia, E.M. Hoek, P. Somasundaran, F. Klaessig, V. Castranova, M. Thompson, Understanding biophysicochemical interactions at the nano-bio interface, Nat. Mater. 8 (7) (2009) 543–557.

[41] S.D. Luthuli, M.M. Chili, N. Revaprasadu, A. Shonhai, Cysteine-capped gold nanoparticles suppress aggregation of proteins exposed to heat stress, IUBMB Life 65 (5) (2013) 454–461.

[42] T. Ruks, C. Beuck, T. Schaller, F.C. Niemeyer, M. Zahres, K. Loza, M. Heggen, U. Hagemann, C. Mayer, P. Bayer, M. Epple, Solution NMR spectroscopy with isotope-labelled cysteine (13C, 15N) reveals the surface structure of L-cysteine-coated ultrasmall gold nanoparticles (1.8 nm), Langmuir (2018).

[43] S. Salatin, S. Maleki Dizaj, A. Yari Khosroushahi, Effect of the surface modification, size, and shape on cellular uptake of nanoparticles, Cell Biol. Int. 39 (8) (2015) 881–890.

[44] E. Frohlich, The role of surface charge in cellular uptake and cytotoxicity of medical nanoparticles, Int. J. Nanomed. 7 (2012) 5577–5591.

[45] L. Caprile, A. Cossaro, E. Falletta, C. Della Pina, O. Cavalleri, R. Rolandi, S. Terreni, R. Ferrando, M. Rossi, L. Floreano, M. Canepa, Interaction of L-cysteine with naked gold nanoparticles supported on Hopg: a high resolution XPS investigation, Nanoscale 4 (24) (2012) 7727–7734.

[46] Z. Chen, A. Bachhuka, S. Han, F. Wei, S. Lu, R.M. Visalakshan, K. Vasilev, Y. Xiao, Tuning chemistry and topography of nanoengineered surfaces to manipulate immune response for bone regeneration applications, ACS Nano 11 (5) (2017) 4494–4506.

[47] R. Lv, Q. Bao, Y. Li, Regulation of M1type and M2type macrophage polarization in RAW264.7 cells by Galectin9, Mol. Med. Rep. 16 (6) (2017) 9111–9119.

[48] F. Kianoush, M. Nematollahi, J.D. Waterfield, D.M. Brunette, Regulation of RAW264.7 macrophage polarization on smooth and rough surface topographies by galectin-3, J. Biomed. Mater. Res. A 105 (9) (2017) 2499–2509.

[49] L.J. Berghaus, J.N. Moore, D.J. Hurley, M.L. Vandenplas, B.P. Fortes, M.A. Wolfert, G.J. Boons, Innate immune responses of primary murine macrophage-lineage cells and RAW 264.7 cells to ligands of Toll-like receptors 2, 3, and 4, Comp. Immunol. Microbiol. Infect. Dis. 33 (5) (2010) 443–454.

[50] R.P. Nishanth, R.G. Jyotsna, J.J. Schlager, S.M. Hussain, P. Reddanna, Inflammatory responses of RAW 264.7 macrophages upon exposure to nanoparticles: role of ROS-NFkappaB signaling pathway, Nanotoxicology 5 (4) (2011) 502–516.

[51] N. Oh, J.H. Park, Surface chemistry of gold nanoparticles mediates their exocytosis in macrophages, ACS Nano 8 (6) (2014) 6232–6241.

[52] K. Nambara, K. Niikura, H. Mitomo, T. Ninomiya, C. Takeuchi, J. Wei, Y. Matsuo, K. Ijiro, Reverse size dependences of the cellular uptake of triangular and spherical gold nanoparticles, Langmuir 32 (47) (2016) 12559–12567.

[53] X. Ma, Y. Wu, S. Jin, Y. Tian, X. Zhang, Y. Zhao, L. Yu, X. Liang, Gold nanoparticles induce autophagosome accumulation through size-dependent nanoparticle uptake and lysosome impairment, ACS Nano 5 (11) (2011) 8629–8639.

[54] N. Tlotleng, M.A. Vetten, F.K. Keter, A. Skepu, R. Tshikhudo, M. Gulumian, Cytotoxicity, intracellular localization and exocytosis of citrate capped and PEG functionalized gold nanoparticles in human hepatocyte and kidney cells, Cell Biol. Toxicol. 32 (4) (2016) 305–321.

[55] D. Bartczak, S. Nitti, T.M. Millar, A.G. Kanaras, Exocytosis of peptide functionalized gold nanoparticles in endothelial cells, Nanoscale 4 (15) (2012) 4470–4472.

[56] A. Sica, M. Erreni, P. Allavena, C. Porta, Macrophage polarization in pathology, Cell. Mol. Life Sci. 72 (21) (2015) 4111–4126.

[57] J.S. Ma, W.J. Kim, J.J. Kim, T.J. Kim, S.K. Ye, M.D. Song, H. Kang, D.W. Kim, W.K. Moon, K.H. Lee, Gold nanoparticles attenuate LPS-induced NO production through the inhibition of NF-kappaB and IFN-beta/STAT1 pathways in RAW264.7 cells, Nitric Oxide 23 (3) (2010) 214–219.

[58] C.Y. Tsai, S.L. Lu, C.W. Hu, C.S. Yeh, G.B. Lee, H.Y. Lei, Size-dependent attenuation of TLR9 signaling by gold nanoparticles in macrophages, J. Immunol. 188 (1) (2012) 68–76.

[59] Z. Liu, W. Li, F. Wang, C. Sun, L. Wang, J. Wang, F. Sun, Enhancement of lipopolysaccharide-induced nitric oxide and interleukin-6 production by PEGylated gold nanoparticles in RAW264.7 cells, Nanoscale 4 (22) (2012) 7135–7142.

[60] H. Cai, P. Yao, Gold nanoparticles with different amino acid surfaces: serum

albumin adsorption, intracellular uptake and cytotoxicity, Colloids Surfaces B Biointerfaces 123 (2014) 900–906.
[61] K. Tsuji, A. Bandyopadhyay, B.D. Harfe, K. Cox, S. Kakar, L. Gerstenfeld, T. Einhorn, C.J. Tabin, V. Rosen, BMP2 activity, although dispensable for bone formation, is required for the initiation of fracture healing, Nat. Genet. 38 (12) (2006) 1424–1429.
[62] Y. Zhang, T. Bose, R.E. Unger, J.A. Jansen, C.J. Kirkpatrick, J. van den Beucken, Macrophage type modulates osteogenic differentiation of adipose tissue MSCs, Cell Tissue Res. 369 (2) (2017) 273–286.
[63] M. Nagata, K. Iwasaki, K. Akazawa, M. Komaki, N. Yokoyama, Y. Izumi, I. Morita, Conditioned medium from periodontal ligament stem cells enhances periodontal regeneration, Tissue Eng. 23 (9–10) (2017) 367–377.
[64] T.S. Rajan, S. Giacoppo, O. Trubiani, F. Diomede, A. Piattelli, P. Bramanti, E. Mazzon, Conditioned medium of periodontal ligament mesenchymal stem cells exert anti-inflammatory effects in lipopolysaccharide-activated mouse motoneurons, Exp. Cell Res. 349 (1) (2016) 152–161.
[65] N. Ma, D. Yang, H. Okamura, J. Teramachi, T. Hasegawa, L. Qiu, T. Haneji, Involvement of interleukin-23 induced by Porphyromonas endodontalis lipopolysaccharide in osteoclastogenesis, Mol. Med. Rep. 15 (2) (2017) 559–566.
[66] Z. Chen, J. Yuen, R. Crawford, J. Chang, C. Wu, Y. Xiao, The effect of osteoimmunomodulation on the osteogenic effects of cobalt incorporated beta-tricalcium phosphate, Biomaterials 61 (2015) 126–138.
[67] C. Wu, Z. Chen, Q. Wu, D. Yi, T. Friis, X. Zheng, J. Chang, X. Jiang, Y. Xiao, Clinoenstatite coatings have high bonding strength, bioactive ion release, and osteoimmunomodulatory effects that enhance in vivo osseointegration, Biomaterials 71 (2015) 35–47.
[68] J. Zhou, Y. Zhang, L. Li, H. Fu, W. Yang, F. Yan, Human beta-defensin 3-combined gold nanoparticles for enhancement of osteogenic differentiation of human periodontal ligament cells in inflammatory microenvironments, Int. J. Nanomed. 13 (2018) 555–567.
[69] O. Takeuchi, S. Akira, Pattern recognition receptors and inflammation, Cell 140 (6) (2010) 805–820.
[70] K. Takeda, S. Akira, Toll-like receptors in innate immunity, Int. Immunol. 17 (1) (2005) 1–14.
[71] E.M.Y. Moresco, D. LaVine, B. Beutler, Toll-like receptors, Curr. Biol. 21 (13) (2011) R488–R493.
[72] C. Guzzo, A. Ayer, S. Basta, B.W. Banfield, K. Gee, IL-27 enhances LPS-induced proinflammatory cytokine production via upregulation of TLR4 expression and signaling in human monocytes, J. Immunol. 188 (2) (2012) 864–873.
[73] M. Muthukuru, R.P. Darveau, TLR signaling that induces weak inflammatory response and SHIP1 enhances osteogenic functions, Bone Res. 2 (2014) 14031.
[74] L.C. Gilbert, J. Rubin, M.S. Nanes, The p55 TNF receptor mediates TNF inhibition of osteoblast differentiation independently of apoptosis, Am. J. Physiol. Endocrinol. Metab. 288 (5) (2005) E1011–E1018.
[75] X. Cao, W. Lin, C. Liang, D. Zhang, F. Yang, Y. Zhang, X. Zhang, J. Feng, C. Chen, Naringin rescued the TNF-α-induced inhibition of osteogenesis of bone marrow-derived mesenchymal stem cells by depressing the activation of NF-κB signaling pathway, Immunol. Res. 62 (3) (2015) 357–367.
[76] C.B. Sullivan, R.M. Porter, C.H. Evans, T. Ritter, G. Shaw, F. Barry, J.M. Murphy, TNFalpha and IL-1beta influence the differentiation and migration of murine MSCs independently of the NF-kappaB pathway, Stem Cell Res. Ther. 5 (4) (2014) 104.
[77] N. Yang, G. Wang, C. Hu, Y. Shi, L. Liao, S. Shi, Y. Cai, S. Cheng, X. Wang, Y. Liu, L. Tang, Y. Ding, Y. Jin, Tumor necrosis factor alpha suppresses the mesenchymal stem cell osteogenesis promoter miR-21 in estrogen deficiency-induced osteoporosis, J. Bone Miner. Res. 28 (3) (2013) 559–573.
[78] S. Kaneshiro, K. Ebina, K. Shi, C. Higuchi, M. Hirao, M. Okamoto, K. Koizumi, T. Morimoto, H. Yoshikawa, J. Hashimoto, IL-6 negatively regulates osteoblast differentiation through the SHP2/MEK2 and SHP2/Akt2 pathways in vitro, J. Bone Miner. Metab. 32 (4) (2014) 378–392.
[79] N. Liu, S. Shi, M. Deng, L. Tang, G. Zhang, N. Liu, B. Ding, W. Liu, Y. Liu, H. Shi, L. Liu, Y. Jin, High levels of beta-catenin signaling reduce osteogenic differentiation of stem cells in inflammatory microenvironments through inhibition of the noncanonical Wnt pathway, J. Bone Miner. Res. 26 (9) (2011) 2082–2095.
[80] Y.L. Wang, H. He, Z.J. Liu, Z.G. Cao, X.Y. Wang, K. Yang, Y. Fang, M. Han, C. Zhang, F.Y. Huo, Effects of TNF-alpha on cementoblast differentiation, mineralization, and apoptosis, J. Dent. Res. 94 (9) (2015) 1225–1232.
[81] C. Yi, D. Liu, C.C. Fong, J. Zhang, M. Yang, Gold nanoparticles promote osteogenic differentiation of mesenchymal stem cells through p38 MAPK pathway, ACS Nano 4 (11) (2010) 6439–6448.
[82] S.Y. Choi, M.S. Song, P.D. Ryu, A.T. Lam, S.W. Joo, S.Y. Lee, Gold nanoparticles promote osteogenic differentiation in human adipose-derived mesenchymal stem cells through the Wnt/beta-catenin signaling pathway, Int. J. Nanomed. 10 (2015) 4383–4392.
[83] J. Li, J.J. Li, J. Zhang, X. Wang, N. Kawazoe, G. Chen, Gold nanoparticle size and shape influence on osteogenesis of mesenchymal stem cells, Nanoscale 8 (15) (2016) 7992–8007.
[84] H. Takayanagi, Osteoimmunology: shared mechanisms and crosstalk between the immune and bone systems, Nat. Rev. Immunol. 7 (4) (2007) 292–304.
[85] U.H. Lerner, Inflammation-induced bone remodeling in periodontal disease and the influence of post-menopausal osteoporosis, J. Dent. Res. 85 (7) (2006) 596–607.
[86] D. Lin, L. Li, Y. Sun, W. Wang, X. Wang, Y. Ye, X. Chen, Y. Xu, IL-17 regulates the expressions of RANKL and OPG in human periodontal ligament cells via TRAF6/TBK1-JNK/NF-kappaB pathways, Immunology (2014).
[87] H. Rizwan, J. Mohanta, S. Si, A. Pal, Gold nanoparticles reduce high glucose-induced oxidative-nitrosative stress regulated inflammation and apoptosis via tuberin-mTOR/NF-kappaB pathways in macrophages, Int. J. Nanomed. 12 (2017) 5841–5862.
[88] S. Ahn, P. Singh, V. Castro-Aceituno, S. Yesmin Simu, Y.J. Kim, R. Mathiyalagan, D.C. Yang, Gold nanoparticles synthesized using Panax ginseng leaves suppress inflammatory - mediators production via blockade of NF-kappaB activation in macrophages, Artif. Cells, Nanomed. Biotechnol. 45 (2) (2017) 270–276.
[89] S. Ahn, P. Singh, M. Jang, Y.J. Kim, V. Castro-Aceituno, S.Y. Simu, Y.J. Kim, D.C. Yang, Gold nanoflowers synthesized using Acanthopanacis cortex extract inhibit inflammatory mediators in LPS-induced RAW264.7 macrophages via NF-kappaB and AP-1 pathways, Colloids Surfaces B Biointerfaces 162 (2018) 398–404.
[90] C. Niu, K. Yuan, R. Ma, L. Gao, W. Jiang, X. Hu, W. Lin, X. Zhang, Z. Huang, Gold nanoparticles promote osteogenic differentiation of human periodontal ligament stem cells via the p38 MAPK signaling pathway, Mol. Med. Rep. 16 (4) (2017) 4879–4886.
[91] D. Zhang, D. Liu, J. Zhang, C. Fong, M. Yang, Gold nanoparticles stimulate differentiation and mineralization of primary osteoblasts through the ERK/MAPK signaling pathway, Materials science & engineering, C, Mater. Biol. Appl. 42 (2014) 70–77.
[92] M. Wei, S. Li, Z. Yang, W. Zheng, W. Le, Gold nanoparticles enhance the differentiation of embryonic stem cells into dopaminergic neurons via mTOR/p70S6K pathway, Nanomedicine (London, England) 12 (11) (2017) 1305–1317.
[93] Y. Pan, Q. Wu, L. Qin, J. Cai, B. Du, Gold nanoparticles inhibit VEGF165-induced migration and tube formation of endothelial cells via the Akt pathway, BioMed Res. Int. 2014 (2014) 418624.
[94] F. Ding, Y. Li, J. Liu, L. Liu, W. Yu, Z. Wang, H. Ni, B. Liu, P. Chen, Overendocytosis of gold nanoparticles increases autophagy and apoptosis in hypoxic human renal proximal tubular cells, Int. J. Nanomed. 9 (2014) 4317–4330.
[95] S. Ke, T. Zhou, P. Yang, Y. Wang, P. Zhang, K. Chen, L. Ren, S. Ye, Gold nanoparticles enhance TRAIL sensitivity through Drp1-mediated apoptotic and autophagic mitochondrial fission in NSCLC cells, Int. J. Nanomed. 12 (2017) 2531–2551.
[96] J.H. Kim, D.E. Lee, J.H. Cha, E.J. Bak, Y.J. Yoo, Receptor activator of nuclear factor-kappaB ligand and sclerostin expression in osteocytes of alveolar bone in rats with ligature-induced periodontitis, J. Periodontol. 85 (11) (2014) e370–e378.
[97] X. Yang, H. Zhang, J. Wang, Z. Zhang, C. Li, Puerarin decreases bone loss and collagen destruction in rats with ligature-induced periodontitis, J. Periodontal. Res. 50 (6) (2015) 748–757.
[98] C. Foureaux Rde, M.R. Messora, L.F. de Oliveira, M.H. Napimoga, A.N. Pereira, M.S. Ferreira, L.J. Pereira, Effects of probiotic therapy on metabolic and inflammatory parameters of rats with ligature-induced periodontitis associated with restraint stress, J. Periodontol. 85 (7) (2014) 975–983.
[99] Y. Matsuda, T. Kato, N. Takahashi, M. Nakajima, K. Arimatsu, T. Minagawa, K. Sato, H. Ohno, K. Yamazaki, Ligature-induced periodontitis in mice induces elevated levels of circulating interleukin-6 but shows only weak effects on adipose and liver tissues, J. Periodontal. Res. 51 (5) (2016) 639–646.
[100] J. Marchesan, M.S. Girnary, L. Jing, M.Z. Miao, S. Zhang, L. Sun, T. Morelli, M.H. Schoenfisch, N. Inohara, S. Offenbacher, Y. Jiao, An experimental murine model to study periodontitis, Nat. Protoc. 13 (10) (2018) 2247–2267.
[101] D. Cui, H. Li, L. Lei, C. Chen, F. Yan, Nonsurgical periodontal treatment reduced aortic inflammation in ApoE(-/-) mice with periodontitis, SpringerPlus 5 (1) (2016) 940.
[102] C. Lopez-Chaves, J. Soto-Alvaredo, M. Montes-Bayon, J. Bettmer, J. Llopis, C. Sanchez-Gonzalez, Gold nanoparticles: distribution, bioaccumulation and toxicity. In vitro and in vivo studies, Nanomed. Nanotechnol. Biol. Med. 14 (1) (2018) 1–12.
[103] S. Hirn, M. Semmler-Behnke, C. Schleh, A. Wenk, J. Lipka, M. Schaffler, S. Takenaka, W. Moller, G. Schmid, U. Simon, W.G. Kreyling, Particle size-dependent and surface charge-dependent biodistribution of gold nanoparticles after intravenous administration, Eur. J. Pharm. Biopharm. 77 (3) (2011) 407–416.
[104] M. Semmler-Behnke, W.G. Kreyling, J. Lipka, S. Fertsch, A. Wenk, S. Takenaka, G. Schmid, W. Brandau, Biodistribution of 1.4- and 18-nm gold particles in rats, Small 4 (12) (2008) 2108–2111.
[105] I. Takeuchi, S. Nobata, N. Oiri, K. Tomoda, K. Makino, Biodistribution and excretion of colloidal gold nanoparticles after intravenous injection: effects of particle size, Bio Med. Mater. Eng. 28 (3) (2017) 315–323.
[106] C. Rambanapasi, J.R. Zeevaart, H. Buntting, C. Bester, D. Kotze, R. Hayeshi, A. Grobler, Bioaccumulation and subchronic toxicity of 14 nm gold nanoparticles in rats, Molecules 21 (6) (2016).
[107] E.A. Nicu, B.G. Loos, Polymorphonuclear neutrophils in periodontitis and their possible modulation as a therapeutic approach, Periodontology 71 (1) (2000) 140–163 (2016).
[108] J.R. Gonzales, T- and B-cell subsets in periodontitis, Periodontology 69 (1) (2000) 181–200 (2015).
[109] M. Zouali, The emerging roles of B cells as partners and targets in periodontitis, Autoimmunity 50 (1) (2017) 61–70.